We would like to thank both referees for their comments regarding our manuscript. Below we have included our responses. The referee comments are in black text while our responses are in blue.

Referee Comment #1

In the study presented in this manuscript, the authors attempt to identify the aerosol components responsible for trends observed in monthly averaged UVAI. Aerosol fields from a global model were combined with radiative transfer calculations to obtain modeled UVAI which were compared with OMI UVAI. Whereas the topic is interesting and the approach promising, the study was not well performed. In particular, I have three major issues with the current manuscript:

1. The interpretation of UVAI and UVAI trends is not sufficiently addressed (as mentioned in the first round of review). The authors have the tools (GCM + RTM) to study the effects of changing aerosol amount, composition, and altitude on UVAI; if they would perform a detailed systematic study for several selected regions (and, possibly, seasons) this would greatly aid the interpretation of observed trends.

We have previously conducted a detailed, systematic study of our simulated UVAI compared to the OMI UVAI for several selected regions and seasons in our previous publication (Hammer et al., 2016; https://doi.org/10.5194/acp-16-2507-2016). We expand on the reference to this previous publication in our introduction:

Page 4 lines 110-112: "In this work, we apply a simulation of the UVAI, which was developed and evaluated regionally and seasonally in Hammer et al. (2016) …"

We also elaborate on our studies of the effects of changing aerosol amount and composition in this manuscript:

Page 12 lines 353-356: "Figure 8 shows the change in annual mean UVAI due to doubling the concentration of individual aerosol species. This information facilitates interpretation of the observed UVAI trends by identifying the chemical components that could explain the observed trends."

and we add new sensitivity simulations of the effects of aerosol altitude:

Page 6 lines 183-186: "We also calculated the change in UVAI due to changes in simulated aerosol altitude, but found that the trends in aerosol altitude were negligible (order 10^{-5} hPa yr^{-1}). Therefore we focus our analysis on trends in aerosol composition which have a larger effect on the UVAI as demonstrated below."

2. The authors attempt to explain observed UVAI trends by comparing with model data that shows rather different trends. It is unclear how this could work.

Indeed we are learning a great deal from the comparison of observed and modelled trends. Our study does not require that our modeled trends match the observed OMI UVAI trends. Rather, in

our UVAI simulation we have known aerosol composition. Therefore we can directly interpret how trends in modelled aerosol composition relate to trends in simulated UVAI values. We can then use the trends in simulated UVAI values with known aerosol composition to interpret either the similarities or differences in the trends in observed OMI UVAI values. This comparison thus offers insight into the observed OMI UVAI values that can be explained by the simulation, and insight into possible explanations of remaining discrepancies.

We write in our introduction:

Page 4 lines 115-118: "Comparison of trends in observed OMI UVAI values to the trends in simulated UVAI values, which are calculated using known aerosol composition, enables qualification of how changes in aerosol absorption and scattering could influence the observed UVAI trends and identification of model development needs."

3. There appears to be no important conclusion. The attribution of various trends to certain changes in aerosol amount or composition remains rather speculative.

We have emphasized that interpretation of the OMI UVAI with a quantitative simulation of the UVAI offers information about trends in aerosol composition. For example, we found that global trends in the UVAI were largely explained by trends in absorption of mineral dust, absorption by brown carbon, and scattering by secondary inorganic aerosols. We also identified areas for model development, such as dust emissions from the desiccating Aral Sea.

Specific comments

Section 5:

a. The presented trends are tiny, at most 0.02 (seen in North Africa) over the whole decade of OMI observations. Although the analysis reports that these trends are statistically significant (as the authors state), I would like to apply to common sense and a critical look at the data: the uncertainty of UVAI is at least on the order of 0.1, and the variability (due to aerosols, clouds, and surface) is much larger. If you insist on discussing these trends, I strongly suggest adding a figure so that the reliability of the trend analysis can be estimated.

Indeed, we have taken great care to address the errors in the UVAI to enable quantitative interpretation of observed trends as now described in line 143. In particular we have uased a recently reprocessed version of the UVAI algorithm which treats clouds with a Mie-scattering based water cloud model. We have used a UVAI algorithm that more accurately accounted for scattering by mineral dust and by clouds, reducing systematic artifacts and scan angle bias. Furthermore, we focus on 10-years of observations so that multiple observations can reduce the random error of UVAI observations.

b. Why is the rather obvious modeled negative trend over the Sahara in SON not addressed in the text? In the conclusions it is mentioned that it is "erroneous", but I'd rather say it is not in agreement with observations (maybe the same trend is present in the observations, but compensated by, e.g., changes in surface reflection).

We have added a comment about the modeled negative trend over the Sahara in SON:

Page 10 lines 308-312: "The simulation underestimates the observed UVAI trend over North Africa in SON, perhaps related to an underestimate in trends in mineral dust emissions in the simulation during this season. He et al. (2014) examined the 2000-2010 trends in global surface albedo using the Global Land Surface Satellites (GLASS) dataset and found no significant trends over this region during SON."

We have rephrased the conclusion:

Page 14 lines 406-408: "The simulated UVAI attributes the positive trends over North Africa to increasing mineral dust, despite an underestimated simulated trend in fall (SON) that deserves further attention."

c. If the dust UVAI over Mongolia decreased due to changes in wind speed, why is this not reproduced by the model?

Our simulation is for a different time period (2005-2015) than the Guan et al. (2017) study over 1960-2007. We have rephrased to emphasize the differences:

Page 11, lines 313-319: "The OMI UVAI trend over Mongolia/Inner Mongolia may be part of a longer term trend. Guan et al. (2017) examined dust storm data over northern China (including Inner Mongolia) for the period 1960-2007, and found that dust storm frequency has been declining over the region due to a gradual decrease in wind speed."

d. As you mention in ll. 321-325, changes in surface reflectance affect the UVAI. This will strongly affect your trend analysis, so it may be important to estimate the contribution of changing surface reflectance to the UVAI trend using VLIDORT.

We have added to the manuscript:

Page 6 lines 179-183: "For the UVAI calculation we use the surface reflectance fields provided by OMI. We calculated the 2005-2015 trends in these surface reflectance fields, and found that they were statistically insignificant globally and on the order of 10^{-5}. We calculated the change in UVAI due to a change in surface reflectance of this order of magnitude, and found that the change in UVAI was negligible. Therefore we focus our analysis on trends in aerosol composition which have a larger effect on the UVAI as demonstrated below."

Section 6:

e. As mentioned in issue 2 above, I fail to see how the comparison of observed trends with model trends can aid the understanding of the observed trends, as there is only little agreement between both data sets. A better set-up for this study would have been a focus on 3-5 regions of interest, for which extensive tests with varying aerosol amounts and composition should have been performed.

Thank you for your suggestion. We prefer to share the full global analysis with the reader for transparency, so the reader can see both areas of agreement and disagreement. We learn from areas of disagreement as much as from areas of agreement as evidenced by the discussion of the feature near the Aral Sea. We elaborate on this in the manuscript:

Page 4 lines 115-118: "Comparison of trends in observed OMI UVAI values to the trends in simulated UVAI values, which are calculated using known aerosol composition, enables qualification of how changes in aerosol absorption and scattering could influence the observed UVAI trends and identification of model development needs."

f. Similarly, it remains unclear what we learn from an analysis as that shown in Fig. 8.

We added:

Page 12 lines 353-356: "Figure 8 shows the change in annual mean UVAI due to doubling the concentration of individual aerosol species. This information facilitates interpretation of the observed UVAI trends by identifying the chemical components that could explain the observed trends."

Section 7:

g. In general, there should be more coupling of the model results to observations. E.g., instead of the inaccurate statement (ll. 408-409) that "The simulation attributed the negative trend over South Asia to increasing scattering secondary inorganic aerosols (...)", I would argue that by comparing Figs. 5, 6, and 9, it can be seen that over India the modeled trend is possibly too small because either the UVAI increase due to more dust is overestimated or the UVAI decrease due to more secondary aerosols is underestimated. The observed trend is negative.

In this revision we have tried to emphasize the coupling of model results to observations. For example, by using scene-dependent OMI viewing geometry together with scene-dependent modelled atmospheric composition we enable quantitative comparison of model results with observations.

Regarding the specific comment for India, the trend in both simulated and observed UVAI values is negative over South Asia. Figure 9 shows that the largest change in our simulated UVAI values over India is a decrease due to the positive trends in scattering SIA over the region. Hence we respectfully retain the statement: "The simulation attributed the negative trend over South Asia to increasing scattering secondary inorganic aerosols, a trend that the observations imply could be even larger."

h. The fact that over the eastern US you find the strongest negative UVAI trend in summer is a strong indication that this is caused by secondary organic aerosols of biogenic origin - not, as stated in the manuscript, SIA. SOA are notoriously badly reproduced by GCMs. (see, e.g., Penning de Vries et al., ACP 2015 (doi: 10.5194/acp-15-10597- 2015))

Good point that OA may play a role. We revised the sentence:

Page 14 lines 415-417: “We found the positive trends in the UVAI over the eastern United States that were strongest in summer (JJA) in both the observations and the simulation were driven by negative trends in scattering secondary inorganic aerosol and organic aerosol.”

We also note that the GEOS-Chem aerosol simulation we use has been extensively evaluated against ground-based PM2.5 composition measurements (Li et al., (2016); DOI: 10.1021/acs.est.7b02530). The simulated aerosol trends were found to well reproduce the summer trends in OA over the southeastern U.S., mainly due to the inclusion of an aqueous formation mechanism of isoprene (Marais et al., 2016; DOI: 10.5194/acp-16-1603-2016).

Minor comments:

p.2, l.42: The indirect effect is only mentioned in passing here, but it is actually at least as great as the direct effect. Please add a line or two about the indirect effect.

We now further emphasize the indirect effect:

Page 2 lines 38-39: “Atmospheric aerosols have significant climate impacts due to their ability to scatter and absorb solar radiation and to their indirect effect through modification of cloud properties.”

p.3, l.64: Please add a reference to the study by Fioletov et al., ACP 2016 (doi: 10.5194/acp-16-11497-2016)

We have added this reference to the revised text:

Page 3 lines 63-66: “Due to the wide implementation of flue-gas desulfurization equipment on most power plants in China, emissions of sulfur dioxide (SO_2) in some regions have been decreasing since about 2006-2008 (Lu et al., 2011; Wang et al., 2015; Fioletov et al., 2016).”

p.4, l.102: Please add a reference to Penning de Vries et al., ACP 2009 after "absorption and scattering." (doi: 10.5194/acp-9-9555-2009)

Done.

p.4, ll.102-105: "Prior interpretation (...) through simulation." This is rather vague. A few more words on UVAI’s "dependence on other parameters" would be helpful here, preferably with a figure showing the AOD and ALH dependences of the different aerosol components (SIA, Dust, OA, BrC, BC, and Salt).

We have rephrased this sentence and have added references to the introduction about these dependencies:

Page 4 lines 105-107: “Prior interpretation of the UVAI has been complicated by its dependence on geophysical parameters, such as aerosol layer height (Herman et al., 1997; Torres et al., 1998; de Graaf et al., 2005).”

In terms of our calculated trends, we calculated the trend in ALH over 2005-2015, and found the trends were ~10^{-5} hPa yr^{-1} in magnitude. We conducted a sensitivity test by calculating the change in UVAI associated with a 1 hPa increase in ALH, and found that gave a negligible change in UVAI (~10^{-6}). As described in the manuscript:

Page 6 lines 183-186: "We also calculated the change in UVAI due to changes in simulated aerosol altitude, but found that the trends in aerosol altitude were negligible (order 10^{-5} hPa yr^{-1}). Therefore we focus our analysis on trends in aerosol composition which have a larger effect on the UVAI as demonstrated below."

p.5, l.128: Add references to Herman et al., 1997, and Torres et al., 1998.

Done.

p.5, ll.133-134: "Negative UVAI values due to aerosol scattering are often weak and buried in noise (Torres et al., 2007)." But certainly not always! In fact, you interpret the negative UVAI values in this study, so please rephrase and cite Penning de Vries et al., ACP 2015 (doi: 10.5194/acp-15-10597-2015)

We have rephrased the sentence and added the citation:

Page 5 lines 137-138: "Negative UVAI values due to aerosol scattering are often weak and have historically been affected by noise in previous datasets (Torres et al., 2007; Penning de Vries et al., 2015)."

p.5, 134-137: "Because UVAI (...) the absorption signal." This statement is too simple; did you test it using your RTM? In fact, multiple scattering (particularly if a layer of scattering aerosols is located below an absorbing aerosol layer) may increase absorption and UVAI.

We have rephrased the sentence:

Page 5 lines 138-141: "Because UVAI values are calculated from top of atmosphere (TOA) radiance which contains total aerosol effects, the presence (or lack) of scattering aerosol along with absorbing aerosol can either weaken (or strengthen) the absorption signal."

We have tested this in the RTM, as shown in Figures 8 and 9.

p.5, ll.139-145: Why do you mention the other OMAERUV products if you don't use them? Consider removing the paragraph. If you do decide to keep it, insert "by incorporating" between "observed radiances" and "aerosol type selection" on line 140.

We have removed the paragraph.

p.5, l.151: Which "cloud fraction" do you mean? Effective? Radiative? The cloud fraction from the UVAI algorithm? How much is 0.05? And a related question: why does so little data over ocean remain - is your cloud filter too restrictive there?

We have clarified in the text that the radiative cloud fraction is from the OMI UVAI algorithm, and 0.05 is 5%. We purposely use a very restrictive cloud filter to reduce error associated with clouds. We clarify this on lines 147-148.

p.6, l.157: "insensitive" -> "less sensitive"

We have made this correction in the revised text.

p.6, l.159: "deseasonalized": this is not mentioned in the results section. Why would you want to do this? More importantly: can you deseasonalize by subtracting a mean value? The UVAI is not additive!

We clarified our objective to focus on the long-term trends. Deseasonalization is a standard method for removing temporal variation from a dataset in order to accurately calculate a long-term trend in a time series. There is no need for the data to be "additive", subtracting the annual mean value from the monthly values allows for the removal of the monthly variation in the UVAI dataset which is not actually due to a trend in the data. This allows focus on long-term UVAI changes over time.

p.6, ll.159-160: "A minimum temporal coverage of 60%": What, exactly, do you mean?

The sentence is rephrased to clarify that a particular pixel must contain data for at least 60% of the time period in order for regression to be performed, to avoid conducting a trend analysis on a pixel where there is only a few years of data.

p.6, ll.177-181: It is unclear to me how the radiances were calculated, can you present an example? E.g., the UVAI of an OMI pixel with 4% cloudiness and cloud optical depth equal to 30 is simulated by summing the radiances from a cloudy pixel with optical depth 30 (Rcloudy) and those from the aerosol scene (Raerosol) by using the independent pixel approximation: Rpixel = 0.04*Rcloudy+0.96*Raerosol But is that approach correct? The cloud fraction determined within the UVAI algorithm is not a real cloud fraction in the sense that it represents cloudiness. It is used by the algorithm to adapt the RT-modeled radiance to the observed radiance. More appropriate would be the use of an independent cloud fraction, e.g. OMI's official cloud product or even MODIS cloud fraction and optical depth (which are available at OMI resolution).

Page 6 lines 175-177: "Following Torres et al. (2018), we compute the radiances used in the UVAI calculation as a combination of clear and cloudy sky conditions. We use the same cloud fractions and cloud optical depths used in the OMI UVAI algorithm for coincident OMI pixels."

An in-depth description of the calculation of the radiances used in the UVAI calculation is provided in Torres et al. (2018) (https://doi.org/10.5194/amt-2017-429).

p.9, ll.260-261: "missing sources of anthropogenic dust": I doubt that, as UVAI is only sensitive to elevated dust layers, see Torres et al., 1998.

The sentence has been rephrased:

Page 9 lines 261-264: “The simulation underestimates some of the smaller dust features captured by OMI, such as over western North America, South America, Australia, and parts of Asia, perhaps reflecting an underestimate in the simulated mineral dust lifetime (Ridley et al. 2012) and missing dust sources (Ginoux et al., 2012; Guan et al., 2016; Huang et al., 2015; Philip et al., 2017).”

p.9, l.274: "OMI,)": spurious comma

We have corrected this in the revised text.

p.9, l.274: "GLS": acronym not explained in the text.

It is explained in the text:

Page 6 lines 158-160: “We perform trend analysis on monthly mean time series data for the years 2005-2015 using Generalized Least Squares (GLS) regression, as described by Boys et al. (2014).”

p. 14, l.418: Please explain the acronym TROPOMI and add a literature reference p. 14, l.420: Please explain the acronym MAIA and add a literature reference

We have added this to the revised text:

Page 14 lines 423-429: “The recent launch of the TROPOspheric Monitoring Instrument (TROPOMI; Veefkind et al., 2012) and the forthcoming geostationary constellation offer UVAI observations at finer spatial and temporal resolution. The forthcoming Multi-Angle Imager for Aerosols (MAIA; Diner et al., 2018) satellite instrument offers an exciting opportunity to derive even more information about aerosol composition by combining measurements at ultraviolet wavelengths with multi-angle observations and polarization sensitivity.”

Referee Comment #2

The paper is appropriate for ACP. I have almost nothing to comment. However, the paper is rather lengthy, like a final report of a project. I can imagine that the information is very useful for many aerosol researchers, especially modelers.

However, if possible the results should be presented in a much more condensed form. Positive as well as negative trends are reported, and a large number of trends are found, at the end the reader is left a bit alone what the main conclusions, what the key messages are.

Thank you for the positive review.

We have emphasized that interpretation of the OMI UVAI with a quantitative simulation of the UVAI offers information about trends in aerosol composition. We write in our introduction:

Page 4 lines 115-118: “Comparison of trends in observed OMI UVAI values to the trends in simulated UVAI values, which are calculated using known aerosol composition, enables

qualification of how changes in aerosol absorption and scattering could influence the observed UVAI trends."

We also identified areas for model development, such as dust emissions from the desiccating Aral Sea.

We have reformatted and condensed some of the text in sections 3 and 5 in a manner which we believe makes the reporting of the UVAI trends easier to follow for the reader.

Insight into Global Trends in Aerosol Composition over 2005-2015 Inferred from the OMI Ultraviolet Aerosol Index

Melanie S. Hammer[1], Randall V. Martin[1,2], Chi Li[1], Omar Torres[3], Max Manning[1], Brian L. Boys[1]

[1]Department of Physics and Atmospheric Science, Dalhousie University, Canada
[2]Harvard-Smithsonian Center for Astrophysics, Cambridge, MA, USA
[3]Atmospheric Chemistry and Dynamics Laboratory, NASA Goddard Space Flight Center, Greenbelt, MD, 20770, USA

Correspondence: melanie.hammer@dal.ca

Abstract

Observations of aerosol scattering and absorption offer valuable information about aerosol composition. We apply a simulation of the Ultraviolet Aerosol Index (UVAI), a method of detecting aerosol absorption from satellite observations, to interpret UVAI values observed by the Ozone Monitoring Instrument (OMI) over 2005-2015 to understand global trends in aerosol composition. We conduct our simulation using the vector radiative transfer model VLIDORT with aerosol fields from the global chemical transport model GEOS-Chem. We examine the 2005-2015 trends in individual aerosol species from GEOS-Chem, and apply these trends to the UVAI simulation to calculate the change in simulated UVAI due to the trends in individual aerosol species. We find that global trends in the UVAI are largely explained by trends in absorption by mineral dust, absorption by brown carbon, and scattering by secondary inorganic aerosol. Trends in absorption by mineral dust dominate the simulated UVAI trends over North Africa, the Middle-East, East Asia, and Australia. The UVAI simulation well resolves observed negative UVAI trends over Australia, but underestimates positive UVAI trends over North Africa and Central Asia near the Aral Sea, and underestimates negative UVAI trends over East Asia. We find evidence of an increasing dust source from the desiccating Aral Sea, that may not be well represented by the current generation of models. Trends in absorption by brown carbon dominate the simulated UVAI trends over biomass burning regions. The UVAI simulation reproduces observed negative trends over central South America and West Africa, but underestimates observed UVAI trends over boreal forests. Trends in scattering by secondary inorganic aerosol dominate the simulated UVAI

trends over the eastern United States and eastern India. The UVAI simulation slightly overestimates the observed positive UVAI trends over the eastern United States, and underestimates the observed negative UVAI trends over India. Quantitative simulation of the OMI UVAI offers new insight into global trends in aerosol composition.

1. Introduction

Atmospheric aerosols have significant climate impacts due to their ability to scatter and absorb solar radiation and to their indirect effect through modification of cloud properties. The exact magnitude of the direct radiative forcing remains highly uncertain (IPCC, 2014), although most studies agree it is significant (Andreae and Gelencsér, 2006; Mann and Emanuel, 2006; Mauritsen, 2016). Storelvmo et al. (2016) estimate that changes in global aerosol loading over the past 45 years have caused cooling (direct and indirect) that masks about one third of the atmospheric warming due to increasing greenhouse gas emissions. Aerosol absorption has been estimated to be the second largest source of atmospheric warming after carbon dioxide (Ramanathan and Carmichael, 2008; Bond et al., 2013; IPCC, 2014), although considerable uncertainty remains regarding the exact magnitude (Stier et al., 2007). The large uncertainty regarding the direct radiative impacts of aerosols on climate is driven by the large variability in aerosol physical and chemical properties, as well as their various emission sources, making it extremely difficult to fully understand their interactions with radiation (Pöschl, 2005; Moosmüller et al., 2009; Curci et al., 2015; Kristiansen et al., 2016). Global observations of trends in aerosol scattering and absorption would offer valuable constraints on trends in aerosol sources and composition.

The emissions of aerosols and their precursors have changed significantly over the past decade. In North America and Europe, the anthropogenic emissions of most aerosol species (e.g. black carbon, organic aerosols) and aerosol precursors (e.g. sulfur dioxide and nitrogen oxides) have decreased due to pollution controls (Leibensperger et al., 2012; Klimont et al., 2013; Curier et al., 2014; Simon et al., 2014; Xing et al., 2015; Li et al., 2017a). By contrast, emissions of aerosols and aerosol precursors have increased in developing countries due to increased industrial activity, particularly in China and India. Chinese emissions of black carbon (BC), organic carbon (OC), and nitrogen oxides (NO_x) have been increasing over the past decade (Zhao et al., 2013; Cui et al., 2015), although in the most recent years NO_x emissions have been declining, driven by

denitration devices at power plants (Liu et al., 2016). Due to the wide implementation of flue-gas desulfurization equipment on most power plants in China, emissions of sulfur dioxide (SO_2) in some regions have been decreasing since about 2006-2008 (Lu et al., 2011; Wang et al., 2015; Fioletov et al., 2016). Indian emissions of anthropogenic aerosols and their precursors have been increasing over the past decade (Lu et al., 2011; Klimont et al., 2017). There have also been significant changes in global dust and biomass burning emissions. Shao et al. (2013) use synoptic data to estimate a global decrease in dust emissions between 1974 and 2012, driven largely by reductions from North Africa with weaker contributions from Northeast Asia, South America, and South Africa. By examining trends in burned area, Giglio et al. (2013) estimate a decrease in global biomass burning emissions between 2000 and 2012. Trends in aerosol composition produced by these changing emissions may be detectable from satellite observations of aerosol scattering and absorption.

Detection of aerosol composition from passive nadir satellite observations is exceedingly difficult; few methods exist. The aerosol-type classification provided by retrievals from the MISR instrument, enabled by multi-angle viewing, is one such source of information about aerosol composition from constraints on particle size, shape, and single scattering albedo (SSA) (Kahn and Gaitley, 2015). MISR retrievals have been used to classify particles relating to events such as biomass burning, desert dust, volcanic eruptions, and pollution events (e.g. Liu et al., 2007; Kalashnikova and Kahn, 2008; Dey and Di Girolamo, 2011; Scollo et al., 2012; Guo et al., 2013). The most commonly used satellite product for aerosol information is aerosol optical depth (AOD), the columnar extinction of radiation by atmospheric aerosols. AOD can be retrieved from satellite measurements of top of atmosphere radiance in combination with prior knowledge of aerosol optical properties. Several studies have examined trends in satellite AOD. Following trends in emissions, over the past decade positive trends in satellite AOD have been observed over Asia and Africa corresponding to regions experiencing industrial growth (de Meij et al., 2012; Chin et al., 2014a; Mao et al., 2014; Mehta et al., 2016), while negative trends in satellite AOD have been observed over North America and Europe, largely due to pollution controls (Hsu et al., 2012; de Meij et al., 2012; Chin et al., 2014b; Mehta et al., 2016). Studies such as these demonstrate the information about the evolution of aerosol abundance offered by total column AOD retrievals, however measurements of absorption would complement the scattering information in AOD retrievals by providing independent information on aerosol composition.

The Ultraviolet Aerosol Index (UVAI) is a method of detecting aerosol absorption from satellite measured radiances (Herman et al., 1997; Torres et al., 1998). Because the UVAI is calculated from measured radiances, a priori assumptions about aerosol composition are not required for its calculation, thus yielding independent information on aerosol scattering (Herman et al., 1997; Torres et al., 1998, 2007; de Graaf et al., 2005; Penning de Vries et al., 2009) and absorption. The UVAI has been widely applied to examine mineral dust (Israelevich et al., 2002; Schepanski et al., 2007; Badarinath et al., 2010; Huang et al., 2010) and biomass burning aerosols (Duncan et al., 2003; Guan et al., 2010; Torres et al., 2010; Kaskaoutis et al., 2011; Mielonen et al., 2012), including brown carbon (Jethva and Torres, 2011; Hammer et al., 2016). The UVAI is not typically used to examine scattering aerosol, however aerosol scattering causes a net decrease in the overall value of the UVAI, meaning that the UVAI could be used to detect changes due to both aerosol absorption and scattering. Prior interpretation of the UVAI has been complicated by its dependence on geophysical parameters, such as aerosol layer height (Herman et al., 1997; Torres et al., 1998; de Graaf et al., 2005). Examining trends in the UVAI would provide an exciting opportunity to investigate the evolution of aerosol absorption and scattering over time, if the multiple parameters affecting the UVAI could be accounted for through simulation.

In this work, we apply a simulation of the UVAI, which was developed and evaluated regionally and seasonally in Hammer et al. (2016), to interpret trends in recently reprocessed OMI UVAI observations for 2005-2015 to understand global changes in aerosol composition. We interpret observed UVAI values by using a radiative transfer model (VLIDORT) to calculate UVAI values as a function of simulated aerosol composition from the global 3-D chemical transport model GEOS-Chem. Comparison of trends in observed OMI UVAI values to the trends in simulated UVAI values, which are calculated using known aerosol composition, enables qualification of how changes in aerosol absorption and scattering could influence the observed UVAI trends and identification of model development needs. We conduct our analysis at the global scale to understand trends worldwide. Section 2 describes the OMI UVAI observations and our UVAI simulation. Section 3 examines the trends in emissions of GEOS-Chem aerosols and their precursors for 2005-2015 to provide context for the trends in our simulated UVAI. Section 4 compares the mean values over 2005-2015 of the OMI UVAI and our simulated UVAI. Section 5 compares the 2005-2015 trends in OMI and simulated UVAI values. In section 6 we examine the sensitivity of the UVAI to changes in the abundance of individual aerosol species. Trends in our

UVAI simulation are interpreted by applying the trends in the GEOS-Chem aerosol species to calculate the associated change in UVAI. Section 7 reports the conclusions.

2. Methods

2.1 OMI Ultraviolet Aerosol Index

The OMI Ultraviolet Aerosol Index is a method of detecting absorbing aerosols from satellite measurements in the near-UV wavelength region and is a product of the OMI Near-UV algorithm (OMAERUV) (Herman et al., 1997; Torres et al., 1998, 2007). The OMAERUV algorithm uses the 354 nm and 388 nm radiances measured by OMI to calculate the UVAI as a measure of the deviation from a purely Rayleigh scattering atmosphere bounded by a Lambertian reflecting surface. Positive UVAI values indicate absorbing aerosol while negative values indicate non-absorbing aerosol. Near-zero values occur when clouds and Rayleigh scattering dominate. Negative UVAI values due to aerosol scattering are often weak and have historically been affected by noise in previous datasets (Torres et al., 2007; Penning de Vries et al., 2015). Because UVAI values are calculated from top of atmosphere (TOA) radiance which contains total aerosol effects, the presence (or lack) of scattering aerosol along with absorbing aerosol can either weaken (or strengthen) the absorption signal. Therefore the UVAI could be used to detect changes over time due to both aerosol absorption and scattering.

In this analysis, we carefully address UVAI error sources to enable quantitative analysis of long term trends. We use a recently reprocessed version of the UVAI algorithm which treats clouds with a Mie-scattering based water cloud model (Torres et al., 2018). This new dataset more accurately accounts for scattering by mineral dust and by clouds, reducing systematic artifacts and scan angle bias. We focus on cloud-filtered observations by excluding scenes with OMI UVAI radiative cloud fraction exceeding 5% to further reduce uncertainty due to clouds. Since 2008 the OMI observations have been affected by a row anomaly which reduces the sensor viewing capability for specific scan angles (http://projects.knmi.nl/omi/research/product/rowanomaly-background.php). The sudden suppression of observations for specific viewing geometries (i.e. the row anomaly), could cause an additional spurious trend in the UVAI calculation. We reduce this concern by using the recently reprocessed OMAERUV UVAI that is less sensitive to scan-angle dependent cloud artifacts and by considering only scan positions 3-23 which remain unaffected by the row anomaly. The monthly time series data are deseasonalized by subtracting the monthly

Deleted: buried in noise

Deleted: will

Deleted: The OMAERUV algorithm also produces retrieved OMI single scattering albedo (SSA) and AOD derived from the observed radiances, aerosol type selection using the OMI UVAI, AIRS carbon monoxide, and aerosol layer height assumptions constrained by climatologies from CALIOP retrievals and a GOCART simulation. These OMI SSA and AOD products have been subjected to rigorous validation studies and have been found to be in reasonable agreement with independent ground-based AOD and SSA inferred from AERONET measurements (Torres et al., 2007, 2013; Ahn et al., 2014; Jethva et al., 2014; Zhang et al., 2016). We focus on the UVAI here since simulation of the UVAI product does not require external information from other satellites or models, and thus enables us to isolate information on aerosol composition.

Deleted: 0.05

Deleted: insensitive

mean for the period 2005-2015 to focus on the long-term trend. Prior to regression, the data is aggregated to monthly mean values, and each pixel is required to have data for at least 60% of the time period in order for regression to be performed. We perform trend analysis on monthly mean time series data for the years 2005-2015 using Generalized Least Squares (GLS) regression, as described by Boys et al. (2014). An additional small, positive, spurious trend in the cloud-filtered OMI UVAI remains which is believed to be due to instrumental effects (Torres et al., 2017). We subtract this spurious global mean trend in the cloud-filtered UVAI prior to interpretation. In the following section, we discuss our UVAI simulation and the implementation of the new UVAI algorithm in the simulation.

2.2 Simulated UVAI

We simulate the UVAI using the VLIDORT radiative transfer model (Spurr, 2006), following Buchard et al. (2015) and Hammer et al. (2016). We calculate the top of atmosphere radiances at 354 nm and 388 nm needed for the UVAI calculation by supplying VLIDORT with the OMI viewing geometry for each scene, as well as the GEOS-Chem simulation of vertical profiles of aerosol extinction, spectrally dependent single scattering albedo, and the corresponding spectrally dependent scattering phase function. Thus these parameters account for the sensitivity of the UVAI to aerosol layer height and spectrally dependent aerosol optical properties.

We introduce to the UVAI simulation a Mie-scattering based water cloud model (Deirmendjian, 1964) for consistency with the reprocessed OMI UVAI dataset. Following Torres et al. (2018), we compute the radiances used in the UVAI calculation as a combination of clear and cloudy sky conditions. We use the same cloud fractions and cloud optical depths used in the OMI UVAI algorithm for coincident OMI pixels. We avoid cloudy scenes by considering only pixels with OMI radiative cloud fraction of less than 5%. For the UVAI calculation we use the surface reflectance fields provided by OMI. We calculated the 2005-2015 trends in these surface reflectance fields, and found that they were statistically insignificant globally and on the order of 10^{-5} yr^{-1}. We calculated the change in UVAI due to a change in surface reflectance of this order of magnitude, and found that the change in UVAI was negligible. We also calculated the change in UVAI due to changes in simulated aerosol altitude, but found that the trends in aerosol altitude were negligible (order 10^{-5} hPa yr^{-1}). Therefore we focus our analysis on trends in aerosol composition which have a larger effect on the UVAI as demonstrated below.

Deleted: 7

We use the GEOS-Chem model v11-01 (http://geos-chem.org) as input to the UVAI simulation, and to calculate the sensitivity of the UVAI simulation to aerosol composition. The simulation is driven by assimilated meteorological data from MERRA-2 Reanalysis of the NASA Global Modeling and Assimilation Office (GMAO). Our simulation is conducted at a spatial resolution of 2° x 2.5° with 47 vertical levels for the years 2005-2015. We supply VLIDORT with GEOS-Chem aerosol fields coincident with OMI observations.

GEOS-Chem contains a detailed oxidant-aerosol chemical mechanism (Bey et al., 2001; Park et al., 2004). The aerosol simulation includes the sulfate-nitrate-ammonium system (Fountoukis and Nenes, 2007; Park et al., 2004; Pye et al., 2009), primary carbonaceous aerosol (Park et al., 2003), mineral dust (Fairlie et al., 2007), and sea salt (Jaeglé et al., 2011). Semivolatile primary organic carbon and secondary organic aerosol formation is described in Pye et al. (2010). We update the original semi-volatile partitioning of secondary OA (SOA) formed from isoprene with the irreversible uptake scheme in Marais et al. (2016). HNO_3 concentrations are reduced following Heald et al. (2012). Aerosol optical properties are based on the Global Aerosol Data Set (GADS) (Koepke et al., 1997) as originally implemented by Martin et al. (2003), with updates for organics and secondary inorganics from aircraft observations (Drury et al., 2010), for mineral dust (Lee et al., 2009; Ridley et al., 2012), and for absorbing brown carbon (Hammer et al., 2016). Here we update the mineral dust optics at ultraviolet wavelengths using a refractive index that minimizes the difference between the mean simulated and OMI UVAI values to allow focus on trends. Aerosols are treated as externally mixed.

Anthropogenic emissions are from the EDGARv4.3.1 global inventory (Crippa et al., 2016) with emissions overwritten in areas with regional inventories for the United States (NEI11;Travis et al., 2016), Canada (CAC), Mexico (BRAVO; Kuhns et al., 2005), Europe (EMEP; http://www.emep.int/), China (MEIC v1.2; Li et al., 2017a) and elsewhere in Asia (MIX; Li et al., 2017a). Emissions from open fires for individual years from the GFED4 inventory (Giglio et al., 2013) are included. The long-term concentrations from this simulation have been extensively evaluated versus ground-based $PM_{2.5}$ composition measurements where available, and versus satellite-derived $PM_{2.5}$ trends (Li et al., 2017b).

The Supplement evaluates trends in simulated SO_2, NO_2, and AOD versus satellite retrievals from multiple instruments and algorithms. We find broad consistency between our simulated NO_2 and SO_2 column trends with those from OMI (Figures S1 and S2). Our simulated

AOD trends are generally consistent with the trends in satellite AOD retrievals, except for positive trends in AOD over western North America and near the Aral Sea in most retrieval products, and a negative trend in AOD over Mongolia/Inner Mongolia in all retrieval products (Figure S3).

We filter our GEOS-Chem aerosol simulated fields based on the coincident OMI pixels, which are regridded to the model resolution of 2° x 2.5°. This allows for the direct comparison between our GEOS-Chem simulation and the OMI UVAI observations.

3. Trend in emissions of GEOS-Chem aerosols and their precursors

Figure 1 shows the trends in emissions of aerosols and their precursors from our GEOS-Chem simulation calculated from the GLS regression of monthly time series values for 2005-2015. Cool colors indicate negative trend values, warm colors indicate positive trend values, and the opacity of the colors indicates the statistical significance of the trends. The trends in emissions of sulfur dioxide (SO_2) and nitrogen oxides (NO_x) follow similar patterns (Figure 1a and 1b, respectively). Negative trends (–1 to -0.01 kg km^{-2} yr^{-1}) are present over North America and Europe, corresponding to pollution controls (Leibensperger et al., 2012; Klimont et al., 2013; Curier et al., 2014; Simon et al., 2014; Xing et al., 2015; Li et al., 2017a). Positive trends (0.5 to 1 kg km^{-2} yr^{-1}) in both species are present over India and eastern China, however the positive trends in emissions of SO_2 over eastern China are interspersed with negative trends (-1 to -0.5 kg km^{-2} yr^{-1}) in SO_2 emissions, corresponding to the deployment of desulfurization equipment on power plants in recent years (Lu et al., 2011; Klimont et al., 2013; Wang et al., 2015). Ammonia (NH_3) emissions (Figure 1c) have positive trends (0.001 to 0.05 kg km^{-2} yr^{-1}) over most of South America, North Africa, the Middle-East, and most of Asia with larger trends (0.1 to 0.5 kg km^{-2} yr^{-1}) over India and eastern China. There are positive trends (0.001 to 0.05 kg km^{-2} yr^{-1}) in black carbon (BC) emissions (Figure 1d) over North Africa, Europe, the Middle-East, India, and China, and negative trends (-0.05 to -0.001 kg km^{-2} yr^{-1}) over North America, Europe, West Africa, and central South America. The trends in primary organic aerosol (POA) emissions (Figure 1e) follow a similar pattern as the trends in BC emissions, except there are negative trends (-0.1 to -0.05 kg km^{-2} yr^{-1}) over eastern China, and the negative trends (-1 to -0.1 kg km^{-2} yr^{-1}) over West Africa and central South America are larger in magnitude reflecting regional changes in fire activity (Chen et al., 2013; Andela and van der Werf, 2014). There are also positive trends (0.001 to 0.05 kg km^{-2} yr^{-1}) over the northern United States and Canada. The trends in dust emissions (Figure 1f) show the

Deleted: Chen et al.2013) found a significant decreasing trend over 2001-2012 using MODIS data in active fires over central South America due to deforestation in Brazil. Using MODIS fire data, Andela and van der Werf (2014) found a declining trend over 2001-2012 in burned area due to cropland expansion over West Africa

largest magnitude of all the various species, although many have low statistical significance, with areas of positive and negative trends (> 1 and < -1 kg km^{-2} yr^{-1}) over North Africa, positive trends (> 1 kg km^{-2} yr^{-1}) parts of the Middle-East, and negative trends (< -1 kg km^{-2} yr^{-1}) over northern China and southern Australia.

4. Mean UVAI values for 2005-2015

We examine the seasonal long-term mean UVAI values for insight into the spatial distribution of the aerosol absorption signals. Figures 2 and 3 show the seasonal mean UVAI values for 2005-2015 for OMI and the simulation, respectively. Positive UVAI values between 0.2 and 1.5 indicating aerosol absorption are present over major desert regions globally for both OMI and the simulation, particularly over the Saharan, Iranian, and Thar deserts. These positive signals are driven by the absorption by mineral dust (Herman et al., 1997; Torres et al., 1998; Buchard et al., 2015). The simulation underestimates some of the smaller dust features captured by OMI, such as over western North America, South America, Australia, and parts of Asia, perhaps reflecting an underestimate in the simulated mineral dust lifetime (Ridley et al. 2012) and missing dust sources (Ginoux et al., 2012; Guan et al., 2016; Huang et al., 2015; Philip et al., 2017). The seasonal variation in the observed and simulated UVAI is similar albeit with larger simulated values in spring (MAM) over North Africa. In all seasons, the UVAI values driven by absorption by dust in the simulation are concentrated mostly over North Africa, while for OMI the UVAI values are more homogeneous over the Middle-East and Asia as well. Positive UVAI values of ~0.2-1 over West and central Africa appearing in both the OMI and simulated values correspond to absorption by brown carbon from biomass burning activities in these regions (Jethva and Torres, 2011; Hammer et al., 2016). Over ocean most data are removed by our strict cloud filter.

5. Trend in UVAI values between 2005-2015

Figure 4 shows the trend in OMI and simulated UVAI values (coincidently sampled from OMI) calculated from the GLS regression of monthly UVAI time series values over 2005-2015. Several regions exhibit consistency between the OMI and simulated UVAI trends. There are statistically significant, positive trends in both OMI and simulated UVAI values over the eastern United States (OMI: 1.0 x10^{-5} to 2.5x10^{-4} yr^{-1}, simulated: 2.5x10^{-4} yr^{-1} to 5.0 x10^{-4} yr^{-1}), and Canada and parts of Russia (OMI: 1.0 x10^{-5} to 2.5x10^{-4} yr^{-1}, simulated: 5.0 x10^{-4} to 2.0x10^{-3} yr^{-1}).

Deleted:

Deleted: Cool colors indicate negative trend values, warm colors indicate positive trend values, and the opacity of the colors indicates the statistical significance of the trends.

Positive UVAI trends (1.0×10^{-5} to 2.5×10^{-4} yr^{-1}) in both OMI and simulated values are present over Europe, although the simulated trends have low statistical significance. Statistically significant, positive UVAI trends (5.0×10^{-4} to 2.0×10^{-3} yr^{-1}) in OMI values are apparent over North Africa, which generally are captured by the simulation but with low statistical significance. Negative UVAI trends (-1.5×10^{-3} yr^{-1} to -1.0×10^{-5} yr^{-1}) in both OMI and simulated values are apparent over most of South America, southern Africa, and Australia. Negative UVAI trends (-2×10^{-3} to -5.0×10^{-4} yr^{-1}) in both OMI and simulated values are present over West Africa, with low statistical significance that could be related to the filtering of persistent clouds. OMI and simulated UVAI values show negative trends (-2×10^{-3} to -5.0×10^{-4} yr^{-1}) over India, although the simulated trends have lower statistical significance.

Deleted: Negative UVAI trendsin both OMI and simulated values are apparent over most of South America, southern Africa, and Australia.

Some regions have trends in OMI UVAI values which are not captured by the simulation. Statistically significant, positive UVAI trends (2.5×10^{-4} yr^{-1} to 1.5×10^{-3} yr^{-1}) over the western United States are apparent in the OMI values but not in the simulation. Zhang et al. (2017) found positive trends in aerosol absorption optical depth from OMI retrievals that they attributed to positive trends in mineral dust over the region, which were not captured by their GEOS-Chem simulation. Statistically significant, positive UVAI trends (5.0×10^{-4} to 2.0×10^{-3} yr^{-1}) in OMI values exist over the Middle-East, while the simulation has negative trends with low statistical significance. The OMI UVAI reveals a region of statistically significant, negative trends (-2×10^{-3} to -5.0×10^{-4} yr^{-1}) over Mongolia/Inner Mongolia which is not captured by the simulation. There is also a small area of statistically significant, positive UVAI trends (1.5×10^{-3} to 2.0×10^{-3} yr^{-1}) in OMI values of over Central Asia between the Caspian Sea and the Aral Sea which is not captured by the simulation. Trends in surface reflectance from the diminishing Aral Sea cannot solely explain the UVAI trends since they extend over the Caspian Sea. Trends in mineral dust are a more likely explanation as discussed further below.

Figures 5 and 6 show the seasonality of the OMI and simulated UVAI trends respectively. The positive UVAI trends over the eastern United States is strongest in summer (JJA) for both OMI and the simulation. The positive UVAI trends over North Africa and the Middle-East are present for all seasons for OMI and for most seasons in the simulation, except in JJA for North Africa and spring (MAM) for the Middle-East. The simulation underestimates the observed UVAI trend over North Africa in SON, perhaps related to an underestimate in trends in mineral dust emissions in the simulation during this season. He et al. (2014) examined the 2000-2010 trends in

global surface albedo using the Global Land Surface Satellites (GLASS) dataset and found no significant trends over this region during SON. The negative trend in UVAI values over West Africa is most apparent in the fall (SON) and winter (DJF) for both OMI and the simulation. The negative OMI UVAI trends over Mongolia/Inner Mongolia and the positive OMI UVAI trends near the Aral Sea are strongest in JJA and weakest in DJF, providing evidence for a mineral dust source. The OMI UVAI trend over Mongolia/Inner Mongolia may be part of a longer term trend. Guan et al. (2017) examined dust storm data over northern China (including Inner Mongolia) for the period 1960-2007, and found that dust storm frequency has been declining over the region due to a gradual decrease in wind speed. The current generation of chemical transport models is unlikely to represent the source near the Aral Sea without an explicit parameterization of the drying sea. The desiccation of the Aral Sea over recent decades has resulted in a steady decline in water coverage over the area (Shi et al., 2014; Shi and Wang, 2015) and has led to the dried up sea bed becoming an increasing source of dust activity in the region (Spivak et al., 2012). Indoitu et al. (2015) found that most dust events are directed towards the west, consistent with the OMI observations. An increase in surface reflectance due to the drying up of the sea bed could also positively influence trends in UVAI. He et al. (2014) found a positive trend over 2000-2010 in surface albedo over the region in JJA and SON, corresponding to when the OMI UVAI trends are strongest.

Deleted: examined the 2000-2010 trends in global surface albedo using the Global Land Surface Satellites (GLASS) dataset and

6. Contribution of individual aerosol species to the simulated UVAI

To further interpret the UVAI trends, we examine the trends in aerosol concentrations from our GEOS-Chem simulation (Figure 7). Figure 7a shows the trends in secondary inorganic aerosol (SIA). There are statistically significant, negative trends over the eastern United States (-1 to -0.05 $\mu g\ m^{-2}\ yr^{-1}$) and statistically significant, positive trends over the Middle-East (0.05 to 0.5 $\mu g\ m^{-2}\ yr^{-1}$), India (0.05 to 1 $\mu g\ m^{-2}\ yr^{-1}$), South America, and southern Africa (0.05 to 0.25 $\mu g\ m^{-2}\ yr^{-1}$). Figure 7b shows the trends in dust. Similar to the trends in emissions, the trends in dust concentrations are of the largest magnitude of the various species, however often with low statistical significance. There are positive trends over the Middle-East (> 2 $\mu g\ m^{-2}\ yr^{-1}$), India (0.05 to 2 $\mu g\ m^{-2}\ yr^{-1}$), and north west China (1 to 2 $\mu g\ m^{-2}\ yr^{-1}$). There are also positive trends (0.05 to 0.25 $\mu g\ m^{-2}\ yr^{-1}$) with low statistical significance over the United States, northern South America, southern Africa, and northern Australia. There is a combination of positive and negative trends (>

2 and < -2 μg m^{-2} yr^{-1}) over North Africa, and negative trends over China and Mongolia (< -2 μg m^{-2} yr^{-1}) and Australia (-1 to -0.5 μg m^{-2} yr^{-1}). Figures 7c and 7d show the trends in total organic aerosol (OA) and the absorbing brown carbon (BrC) component of OA, respectively. Positive trends over Canada and parts of Russia (0.05 to 0.5 μg m^{-2} yr^{-1}) in total OA are mainly due to the positive trend in BrC. Statistically significant, negative trends in total OA (-1 to -0.05 μg m^{-2} yr^{-1}) over the eastern United States are dominated by scattering organic aerosol. Statistically significant, negative trends (-2 to -0.05 μg m^{-2} yr^{-1}) over West Africa and South America for total OA are dominated by the trend in absorbing BrC. Figures 5e and 5f show the trends in black carbon (BC) and salt, respectively. There are positive trends (0.05 to 0.25 μg m^{-2} yr^{-1}) in BC with low statistical significance over India and China. Sea salt trends are negligible.

To gain further insight into how changes in aerosols effect the trends in simulated UVAI, we examine the sensitivity of the UVAI to changes in individual aerosol species. Figure 8 shows the change in annual mean UVAI due to doubling the concentration of individual aerosol species. This information facilitates interpretation of the observed UVAI trends by identifying the chemical components that could explain the observed trends. Doubling scattering SIA concentrations (Figure 8a) decreases the UVAI between -0.25 and -0.1 over most of the globe, with the largest changes over the Eastern United States, Europe, parts of the Middle-East, India, and south east China. Doubling dust concentrations (Figure 8b) produces the largest changes in UVAI, causing increases between 0.5 and 1 over North Africa, and smaller increases between 0.2 and 0.5 over the Middle-East, Europe, and parts of Asia and Australia. Figures 8c and 8d show the changes in UVAI due to doubling total OA concentrations and the absorbing BrC component, respectively. The doubling of BrC increases the UVAI between 0.1 and 0.5 over Canada, West and central Africa, India, parts of Russia, eastern China, and central South America. Doubling total OA concentrations over central South America causes a net decrease of ~ -0.1 as the scattering component of total OA cancels out the absorption by BrC. Doubling BC concentrations (Figure 8e) increases the UVAI of 0.1 over central Africa, India, and south east China, while doubling sea salt concentrations (Figure 8f) has negligible effect on the UVAI.

Figure 9 shows the change in simulated UVAI due to the 2005-2015 trends in individual aerosol species from our GEOS-Chem simulation. The change for each species is calculated by applying the aerosol concentration trends for the individual aerosol type while leaving the concentrations unchanged for the other aerosol species, then taking the difference between this

perturbed UVAI simulation and an unperturbed simulation. Negative trends in scattering SIA (Figure 9a) increase the UVAI by $1.0x10^{-4}$ to $7.5x10^{-3}$ yr^{-1} over the eastern United States and by $1.0x10^{-4}$ to $2.5x10^{-3}$ yr^{-1} over Europe, corresponding to regions of positive UVAI trends in both OMI and the simulation (Figure 4). Increasing SIA decreases the UVAI by $-2.5x10^{-3}$ yr^{-1} to $-1.0x10^{-4}$ yr^{-1} over the Middle-East, India, and east China. Trends in dust concentrations (Figure 9b) cause the largest change in UVAI with regional increases $> 1x10^{-2}$ yr^{-1} and regional decreases $< -1x10^{-2}$ yr^{-1}. Simulated UVAI trends due to mineral dust are mostly negative over North Africa, East Asia, and Australia, while mostly positive over the Middle-East. Noisy trends in regional meteorology cause heterogeneous trends in dust and in the UVAI, with low statistical significance. Figures 9c and 9d show the change in UVAI due to the trends in total OA and the absorbing BrC component of total OA, respectively. Most of the changes in UVAI due to the trends in total OA are caused by the trends in the absorbing BrC component, with increases in the UVAI between $2.5x10^{-3}$ and $1x10^{-2}$ yr^{-1} over Canada and parts of Russia, corresponding to regions of positive UVAI trends for both OMI and the simulation (Figure 4). There are decreases in the UVAI $< -1x10^{-2}$ yr^{-1} over central South America and West Africa due to the negative trends in BrC, corresponding to regions of negative UVAI trends for both OMI and the simulation (Figure 4). Over the eastern United States there is a mixture of increases and decreases in the UVAI due to the trends in scattering organic aerosol. Positive trends in BC increase the UVAI (Figure 9e) by $1.0x10^{-4}$ to $2.5x10^{-3}$ yr^{-1} over India and China. There are no obvious changes in the UVAI due to the trends in sea salt (Figure 9f).

7. Conclusions

Observations of aerosol scattering and absorption offer valuable information about aerosol composition. We simulated the Ultraviolet Aerosol Index (UVAI), a method of detecting aerosol absorption using satellite measurements, to interpret trends in OMI observed UVAI over 2005-2015 to understand global trends in aerosol composition. We conducted our simulation using the vector radiative transfer model VLIDORT with aerosol fields from the global chemical transport model GEOS-Chem.

We examined the 2005-2015 trends in individual aerosol species from GEOS-Chem, and applied these trends to the UVAI simulation to calculate the change in simulated UVAI due to the trends in individual aerosol species. We found that global trends in the UVAI were largely

explained by trends in absorption by mineral dust, absorption by brown carbon, and scattering by secondary inorganic aerosols. The two most prominent positive trends in the observed UVAI were over North Africa and over Central Asia near the desiccating Aral Sea. The simulated UVAI attributes the positive trends over North Africa to increasing mineral dust, despite an underestimated simulated trend in fall (SON) that deserves further attention. The positive trends in the observed UVAI over Central Asia near the shrinking Aral Sea are likely due to increased dust emissions, a feature that is unlikely to be represented in most chemical transport models. The most prominent negative trends in the observed UVAI were over East Asia, South Asia, and Australia. The simulation attributed the negative trends over East Asia and Australia to decreasing mineral dust, despite underestimating the trend in East Asia. The simulation attributed the negative trend over South Asia to increasing scattering secondary inorganic aerosols, a trend that the observations imply could be even larger. We found the positive trends in the UVAI over the eastern United States that were strongest in summer (JJA) in both the observations and the simulation were driven by negative trends in scattering secondary inorganic aerosol and organic aerosol. Observed negative trends in winter (DJF) were less well simulated. Over West Africa and South America, negative trends in UVAI were explained by negative trends in absorbing brown carbon. Thus, trends in the observed UVAI offer valuable information on the evolution of global aerosol composition that can be understood through quantitative simulation of the UVAI. Looking forward, the availability of the UVAI observations from 1979 to the present offer a unique opportunity to understand long-term trends in aerosol composition. The recent launch of the TROPOspheric Monitoring Instrument (TROPOMI; Veefkind et al., 2012) and the forthcoming geostationary constellation offer UVAI observations at finer spatial and temporal resolution. The forthcoming Multi-Angle Imager for Aerosols (MAIA; Diner et al., 2018) satellite instrument offers an exciting opportunity to derive even more information about aerosol composition by combining measurements at ultraviolet wavelengths with multi-angle observations and polarization sensitivity.

Deleted: erroneous

Deleted: negative

Deleted: (SIA)

Acknowledgements

This work was supported by the Natural Science and Engineering Research Council of Canada and the Killam Trusts. Computational facilities were provided in part by the Atlantic Computational Excellence Network and the Graham consortiums of Compute Canada.

505 **References**

506 Andela, N. and van der Werf, G. R.: Recent trends in African fires driven by cropland expansion
507 and El Niño to La Niña transition, Nat. Clim. Chang., 4(9), 791–795, doi:10.1038/nclimate2313,
508 2014.

509 Andreae, M. O. and Gelencsér, A.: Black carbon or brown carbon? The nature of light-absorbing
510 carbonaceous aerosols, Atmos. Chem. Phys., 6(10), 3131–3148, doi:10.5194/acp-6-3131-2006,
511 2006.

512 Badarinath, K. V. S., Kharol, S. K., Kaskaoutis, D. G., Sharma, A. R., Ramaswamy, V. and
513 Kambezidis, H. D.: Long-range transport of dust aerosols over the Arabian Sea and Indian region
514 — A case study using satellite data and ground-based measurements, Glob. Planet. Change, 72(3),
515 164–181, doi:10.1016/j.gloplacha.2010.02.003, 2010.

516 Bey, I., Jacob, D. J., Yantosca, R. M., Logan, J. A., Field, B. D., Fiore, A. M., Li, Q., Liu, H. Y.,
517 Mickley, L. J. and Schultz, M. G.: Global modeling of tropospheric chemistry with assimilated
518 meteorology: Model description and evaluation, J. Geophys. Res., 106(D19), 23073,
519 doi:10.1029/2001JD000807, 2001.

520 Bond, T. C., Doherty, S. J., Fahey, D. W., Forster, P. M., Berntsen, T., DeAngelo, B. J., Flanner,
521 M. G., Ghan, S., Kärcher, B., Koch, D., Kinne, S., Kondo, Y., Quinn, P. K., Sarofim, M. C.,
522 Schultz, M. G., Schulz, M., Venkataraman, C., Zhang, H., Zhang, S., Bellouin, N., Guttikunda, S.
523 K., Hopke, P. K., Jacobson, M. Z., Kaiser, J. W., Klimont, Z., Lohmann, U., Schwarz, J. P.,
524 Shindell, D., Storelvmo, T., Warren, S. G. and Zender, C. S.: Bounding the role of black carbon in
525 the climate system: A scientific assessment, J. Geophys. Res. Atmos., 118(11), 5380–5552,
526 doi:10.1002/jgrd.50171, 2013.

527 Boys, B. L., Martin, R. V., van Donkelaar, A., MacDonell, R. J., Hsu, N. C., Cooper, M. J.,
528 Yantosca, R. M., Lu, Z., Streets, D. G., Zhang, Q. and Wang, S. W.: Fifteen-Year Global Time
529 Series of Satellite-Derived Fine Particulate Matter, Environ. Sci. Technol., 48(19), 11109–11118,
530 doi:10.1021/es502113p, 2014.

531 Buchard, V., da Silva, A. M., Colarco, P. R., Darmenov, A., Randles, C. A., Govindaraju, R.,
532 Torres, O., Campbell, J. and Spurr, R.: Using the OMI aerosol index and absorption aerosol optical
533 depth to evaluate the NASA MERRA Aerosol Reanalysis, Atmos. Chem. Phys., 15(10), 5743–
534 5760, doi:10.5194/acp-15-5743-2015, 2015.

535 Chen, Y., Morton, D. C., Jin, Y., Collatz, G. J., Kasibhatla, P. S., van der Werf, G. R., DeFries, R.
536 S. and Randerson, J. T.: Long-term trends and interannual variability of forest, savanna and
537 agricultural fires in South America, Carbon Manag., 4(6), 617–638, doi:10.4155/cmt.13.61, 2013.

538 Chin, M., Diehl, T., Tan, Q., Prospero, J. M., Kahn, R. A., Remer, L. A., Yu, H., Sayer, A. M.,
539 Bian, H., Geogdzhayev, I. V., Holben, B. N., Howell, S. G., Huebert, B. J., Hsu, N. C., Kim, D.,
540 Kucsera, T. L., Levy, R. C., Mishchenko, M. I., Pan, X., Quinn, P. K., Schuster, G. L., Streets, D.
541 G., Strode, S. A., Torres, O. and Zhao, X.-P.: Multi-decadal aerosol variations from 1980 to 2009:
542 a perspective from observations and a global model, Atmos. Chem. Phys., 14(7), 3657–3690,
543 doi:10.5194/acp-14-3657-2014, 2014a.

544 Chin, M., Diehl, T., Tan, Q., Prospero, J. M., Kahn, R. A., Remer, L. A., Yu, H., Sayer, A. M.,
545 Bian, H., Geogdzhayev, I. V., Holben, B. N., Howell, S. G., Huebert, B. J., Hsu, N. C., Kim, D.,
546 Kucsera, T. L., Levy, R. C., Mishchenko, M. I., Pan, X., Quinn, P. K., Schuster, G. L., Streets, D.

G., Strode, S. A., Torres, O. and Zhao, X.-P.: Multi-decadal aerosol variations from 1980 to 2009: a perspective from observations and a global model, Atmos. Chem. Phys., 14(7), 3657–3690, doi:10.5194/acp-14-3657-2014, 2014b.

Crippa, M., Janssens-Maenhout, G., Dentener, F., Guizzardi, D., Sindelarova, K., Muntean, M., Van Dingenen, R. and Granier, C.: Forty years of improvements in European air quality: regional policy-industry interactions with global impacts, Atmos. Chem. Phys., 16(6), 3825–3841, doi:10.5194/acp-16-3825-2016, 2016.

Cui, H., Mao, P., Zhao, Y., Nielsen, C. P. and Zhang, J.: Patterns in atmospheric carbonaceous aerosols in China: emission estimates and observed concentrations, Atmos. Chem. Phys., 15(15), 8657–8678, doi:10.5194/acp-15-8657-2015, 2015.

Curci, G., Hogrefe, C., Bianconi, R., Im, U., Balzarini, A., Baró, R., Brunner, D., Forkel, R., Giordano, L., Hirtl, M., Honzak, L., Jiménez-Guerrero, P., Knote, C., Langer, M., Makar, P. A., Pirovano, G., Pérez, J. L., San José, R., Syrakov, D., Tuccella, P., Werhahn, J., Wolke, R., Žabkar, R., Zhang, J. and Galmarini, S.: Uncertainties of simulated aerosol optical properties induced by assumptions on aerosol physical and chemical properties: An AQMEII-2 perspective, Atmos. Environ., 115, 541–552, doi:10.1016/j.atmosenv.2014.09.009, 2015.

Curier, L., Kranenburg, R., Timmermans, R., Segers, A., Eskes, H. and Schaap, M.: Synergistic Use of LOTOS-EUROS and NO2 Tropospheric Columns to Evaluate the NOX Emission Trends Over Europe, pp. 239–245., 2014.

Deirmendjian, D.: Scattering and Polarization Properties of Water Clouds and Hazes in the Visible and Infrared, Appl. Opt., 3(2), 187, doi:10.1364/AO.3.000187, 1964.

Dey, S. and Di Girolamo, L.: A decade of change in aerosol properties over the Indian subcontinent, Geophys. Res. Lett., 38(14), n/a-n/a, doi:10.1029/2011GL048153, 2011.

Diner, D. J., Brauer, M., Bruegge, C., Burke, K. A., Chipman, R., Di Girolamo, L., Garay, M. J., Hasheminassab, S., Hyer, E., Jerrett, M., Jovanovic, V., Kalashnikova, O. V., Liu, Y., Lyapustin, A. I., Martin, R. V., Nastan, A., Ostro, B. D., Ritz, B., Schwartz, J., Wang, J. and Xua, F.: Advances in multiangle satellite remote sensing of speciated airborne particulate matter and association with adverse health effects: from MISR to MAIA, J. Appl. Rem. Sens.., Submitted, 2018.

Drury, E., Jacob, D. J., Spurr, R. J. D., Wang, J., Shinozuka, Y., Anderson, B. E., Clarke, A. D., Dibb, J., McNaughton, C. and Weber, R.: Synthesis of satellite (MODIS), aircraft (ICARTT), and surface (IMPROVE, EPA-AQS, AERONET) aerosol observations over eastern North America to improve MODIS aerosol retrievals and constrain surface aerosol concentrations and sources, J. Geophys. Res., 115(D14), D14204, doi:10.1029/2009JD012629, 2010.

Duncan, B. N., Martin, R. V., Staudt, A. C., Yevich, R. and Logan, J. A.: Interannual and seasonal variability of biomass burning emissions constrained by satellite observations, J. Geophys. Res., 108(D2), 4100, doi:10.1029/2002JD002378, 2003.

Fairlie, D. J., Jacob, D. J. and Park, R. J.: The impact of transpacific transport of mineral dust in the United States, Atmos. Environ., 41(6), 1251–1266, doi:10.1016/j.atmosenv.2006.09.048, 2007.

Fioletov, V. E., McLinden, C. A., Krotkov, N., Li, C., Joiner, J., Theys, N., Carn, S. and Moran, M. D.: A global catalogue of large SO2 sources and emissions derived from the Ozone Monitoring Instrument, Atmos. Chem. Phys., 16(18), 11497–11519, doi:10.5194/acp-16-11497-2016, 2016.

Fountoukis, C. and Nenes, A.: ISORROPIA II: a computationally efficient thermodynamic equilibrium model for K^+–Ca^{2+}–Mg^{2+}–NH_4^+–Na^+–SO_4^{2-}–NO_3^-–Cl^-–H_2O aero, Atmos. Chem. Phys., 7(17), 4639–4659, doi:10.5194/acp-7-4639-2007, 2007.

Giglio, L., Randerson, J. T. and van der Werf, G. R.: Analysis of daily, monthly, and annual burned area using the fourth-generation global fire emissions database (GFED4), J. Geophys. Res. Biogeosciences, 118(1), 317–328, doi:10.1002/jgrg.20042, 2013.

Ginoux, P., Prospero, J. M., Gill, T. E., Hsu, N. C. and Zhao, M.: Global-scale attribution of anthropogenic and natural dust sources and their emission rates based on MODIS Deep Blue aerosol products, Rev. Geophys., 50(3), doi:10.1029/2012RG000388, 2012.

de Graaf, M., Stammes, P., Torres, O. and Koelemeijer, R. B. A.: Absorbing Aerosol Index: Sensitivity analysis, application to GOME and comparison with TOMS, J. Geophys. Res., 110(D1), D01201, doi:10.1029/2004JD005178, 2005.

Guan, H., Esswein, R., Lopez, J., Bergstrom, R., Warnock, A., Follette-Cook, M., Fromm, M. and Iraci, L. T.: A multi-decadal history of biomass burning plume heights identified using aerosol index measurements, Atmos. Chem. Phys., 10(14), 6461–6469, doi:10.5194/acp-10-6461-2010, 2010.

Guan, Q., Sun, X., Yang, J., Pan, B., Zhao, S., Wang, L., Guan, Q., Sun, X., Yang, J., Pan, B., Zhao, S. and Wang, L.: Dust Storms in Northern China: Long-Term Spatiotemporal Characteristics and Climate Controls, J. Clim., 30(17), 6683–6700, doi:10.1175/JCLI-D-16-0795.1, 2017.

Guan, X., Huang, J., Zhang, Y., Xie, Y. and Liu, J.: The relationship between anthropogenic dust and population over global semi-arid regions, Atmos. Chem. Phys., 16(8), 5159–5169, doi:10.5194/acp-16-5159-2016, 2016.

Guo, Y., Tian, B., Kahn, R. A., Kalashnikova, O., Wong, S. and Waliser, D. E.: Tropical Atlantic dust and smoke aerosol variations related to the Madden-Julian Oscillation in MODIS and MISR observations, J. Geophys. Res. Atmos., 118(10), 4947–4963, doi:10.1002/jgrd.50409, 2013.

Hammer, M. S., Martin, R. V., van Donkelaar, A., Buchard, V., Torres, O., Ridley, D. A. and Spurr, R. J. D.: Interpreting the ultraviolet aerosol index observed with the OMI satellite instrument to understand absorption by organic aerosols: implications for atmospheric oxidation and direct radiative effects, Atmos. Chem. Phys., 16(4), 2507–2523, doi:10.5194/acp-16-2507-2016, 2016.

He, T., Liang, S. and Song, D.-X.: Analysis of global land surface albedo climatology and spatial-temporal variation during 1981-2010 from multiple satellite products, J. Geophys. Res. Atmos., 119(17), 10,281-10,298, doi:10.1002/2014JD021667, 2014.

Heald, C. L., J. L. Collett Jr., J. L., Lee, T., Benedict, K. B., Schwandner, F. M., Li, Y., Clarisse, L., Hurtmans, D. R., Van Damme, M., Clerbaux, C., Coheur, P.-F., Philip, S., Martin, R. V. and Pye, H. O. T.: Atmospheric ammonia and particulate inorganic nitrogen over the United States, Atmos. Chem. Phys., 12(21), 10295–10312, doi:10.5194/acp-12-10295-2012, 2012.

Herman, J. R., Bhartia, P. K., Torres, O., Hsu, C., Seftor, C. and Celarier, E.: Global distribution of UV-absorbing aerosols from Nimbus 7/TOMS data, J. Geophys. Res., 102(D14), 16911, doi:10.1029/96JD03680, 1997.

Hsu, N. C., Gautam, R., Sayer, A. M., Bettenhausen, C., Li, C., Jeong, M. J., Tsay, S.-C. and Holben, B. N.: Global and regional trends of aerosol optical depth over land and ocean using SeaWiFS measurements from 1997 to 2010, Atmos. Chem. Phys. Atmos. Chem. Phys., 12, 8037–8053, doi:10.5194/acp-12-8037-2012, 2012.

Huang, J., Minnis, P., Yan, H., Yi, Y., Chen, B., Zhang, L. and Ayers, J. K.: Dust aerosol effect on semi-arid climate over Northwest China detected from A-Train satellite measurements, Atmos. Chem. Phys., 10(14), 6863–6872, doi:10.5194/acp-10-6863-2010, 2010.

Huang, J. P., Liu, J. J., Chen, B. and Nasiri, S. L.: Detection of anthropogenic dust using CALIPSO lidar measurements, Atmos. Chem. Phys., 15(20), 11653–11665, doi:10.5194/acp-15-11653-2015, 2015.

Indoitu, R., Kozhoridze, G., Batyrbaeva, M., Vitkovskaya, I., Orlovsky, N., Blumberg, D. and Orlovsky, L.: Dust emission and environmental changes in the dried bottom of the Aral Sea, Aeolian Res., 17, 101–115, doi:10.1016/j.aeolia.2015.02.004, 2015.

IPCC: Climate Change 2014: Impacts, Adaptation, and Vulnerability. Part A: Global and Sectoral Aspects. Contribution of Working Group II to the Fifth Assessment Report of the Intergovernmental Panel on Climate Change [Field, C.B., V.R. Barros, D.J. Dokken, K.J., Cambridge University Press, Cambridge, United Kingdom and New York, NY, USA., 2014.

Israelevich, P. L., Levin, Z., Joseph, J. H. and Ganor, E.: Desert aerosol transport in the Mediterranean region as inferred from the TOMS aerosol index, J. Geophys. Res. Atmos., 107(D21), AAC 13-1-AAC 13-13, doi:10.1029/2001JD002011, 2002.

Jaeglé, L., Quinn, P. K., Bates, T. S., Alexander, B. and Lin, J.-T.: Global distribution of sea salt aerosols: new constraints from in situ and remote sensing observations, Atmos. Chem. Phys., 11(7), 3137–3157, doi:10.5194/acp-11-3137-2011, 2011.

Jethva, H. and Torres, O.: Satellite-based evidence of wavelength-dependent aerosol absorption in biomass burning smoke inferred from Ozone Monitoring Instrument, Atmos. Chem. Phys., 11(20), 10541–10551, doi:10.5194/acp-11-10541-2011, 2011.

Kahn, R. A. and Gaitley, B. J.: An analysis of global aerosol type as retrieved by MISR, J. Geophys. Res. Atmos., 120(9), 4248–4281, doi:10.1002/2015JD023322, 2015.

Kalashnikova, O. V. and Kahn, R. A.: Mineral dust plume evolution over the Atlantic from MISR and MODIS aerosol retrievals, J. Geophys. Res., 113(D24), D24204, doi:10.1029/2008JD010083, 2008.

Kaskaoutis, D. G., Kharol, S. K., Sifakis, N., Nastos, P. T., Sharma, A. R., Badarinath, K. V. S. and Kambezidis, H. D.: Satellite monitoring of the biomass-burning aerosols during the wildfires of August 2007 in Greece: Climate implications, Atmos. Environ., 45(3), 716–726, doi:10.1016/j.atmosenv.2010.09.043, 2011.

Klimont, Z., Smith, S. J. and Cofala, J.: The last decade of global anthropogenic sulfur dioxide: 2000–2011 emissions, Environ. Res. Lett. Environ. Res. Lett, 8(8), 14003–6, doi:10.1088/1748-9326/8/1/014003, 2013.

Klimont, Z., Kupiainen, K., Heyes, C., Purohit, P., Cofala, J., Rafaj, P., Borken-Kleefeld, J. and Schöpp, W.: Global anthropogenic emissions of particulate matter including black carbon, Atmos. Chem. Phys., 17(14), 8681–8723, doi:10.5194/acp-17-8681-2017, 2017.

Koepke, P., Hess, M., Schult, I. and Shettle, E. P.: Global Aerosol Dataset, report, Max-Planck Inst. fur Meteorol., Hamburg, Germany., 1997.

Kristiansen, N. I., Stohl, A., Olivié, D. J. L., Croft, B., Søvde, O. A., Klein, H., Christoudias, T., Kunkel, D., Leadbetter, S. J., Lee, Y. H., Zhang, K., Tsigaridis, K., Bergman, T., Evangeliou, N., Wang, H., Ma, P.-L., Easter, R. C., Rasch, P. J., Liu, X., Pitari, G., Di Genova, G., Zhao, S. Y., Balkanski, Y., Bauer, S. E., Faluvegi, G. S., Kokkola, H., Martin, R. V., Pierce, J. R., Schulz, M., Shindell, D., Tost, H. and Zhang, H.: Evaluation of observed and modelled aerosol lifetimes using radioactive tracers of opportunity and an ensemble of 19 global models, Atmos. Chem. Phys., 16(5), 3525–3561, doi:10.5194/acp-16-3525-2016, 2016.

Kuhns, H., Knipping, E. M. and Vukovich, J. M.: Development of a United States–Mexico Emissions Inventory for the Big Bend Regional Aerosol and Visibility Observational (BRAVO) Study, J. Air Waste Manage. Assoc., 55(5), 677–692, doi:10.1080/10473289.2005.10464648, 2005.

Lee, C., Martin, R. V., van Donkelaar, A., O'Byrne, G., Krotkov, N., Richter, A., Huey, L. G. and Holloway, J. S.: Retrieval of vertical columns of sulfur dioxide from SCIAMACHY and OMI: Air mass factor algorithm development, validation, and error analysis, J. Geophys. Res., 114(D22), D22303, doi:10.1029/2009JD012123, 2009.

Leibensperger, E. M., Mickley, L. J., Jacob, D. J., Chen, W.-T., Seinfeld, J. H., Nenes, A., Adams, P. J., Streets, D. G., Kumar, N. and Rind, D.: Climatic effects of 1950–2050 changes in US anthropogenic aerosols – Part 2: Climate response, Atmos. Chem. Phys., 12(7), 3349–3362, doi:10.5194/acp-12-3349-2012, 2012.

Li, C., Martin, R. V., van Donkelaar, A., Boys, B. L., Hammer, M. S., Xu, J.-W., Marais, E. A., Reff, A., Strum, M., Ridley, D. A., Crippa, M., Brauer, M. and Zhang, Q.: Trends in Chemical Composition of Global and Regional Population-Weighted Fine Particulate Matter Estimated for 25 Years, Environ. Sci. Technol., acs.est.7b02530, doi:10.1021/acs.est.7b02530, 2017a.

Li, M., Zhang, Q., Kurokawa, J., Woo, J.-H., He, K., Lu, Z., Ohara, T., Song, Y., Streets, D. G., Carmichael, G. R., Cheng, Y., Hong, C., Huo, H., Jiang, X., Kang, S., Liu, F., Su, H. and Zheng, B.: MIX: a mosaic Asian anthropogenic emission inventory under the international collaboration framework of the MICS-Asia and HTAP, Atmos. Chem. Phys., 17(2), 935–963, doi:10.5194/acp-17-935-2017, 2017b.

Liu, F., Zhang, Q., van der A, R. J., Zheng, B., Tong, D., Yan, L., Zheng, Y. and He, K.: Recent reduction in NO_x emissions over China: synthesis of satellite observations and emission inventories, Environ. Res. Lett., 11(11), 114002, doi:10.1088/1748-9326/11/11/114002, 2016.

Liu, Y., Koutrakis, P. and Kahn, R.: Estimating fine particulate matter component concentrations and size distributions using satellite-retrieved fractional aerosol optical depth: part 1--method development., J. Air Waste Manag. Assoc., 57(11), 1351–9 [online] Available from: http://www.ncbi.nlm.nih.gov/pubmed/18069458 (Accessed 6 September 2017), 2007.

Lu, Z., Zhang, Q. and Streets, D. G.: Sulfur dioxide and primary carbonaceous aerosol emissions in China and India, Atmos. Chem. Phys. Atmos. Chem. Phys., 11, 9839–9864, doi:10.5194/acp-11-9839-2011, 2011.

Mann, M. E. and Emanuel, K. A.: Atlantic hurricane trends linked to climate change, Eos, Trans. Am. Geophys. Union, 87(24), 233, doi:10.1029/2006EO240001, 2006.

Mao, K. B., Ma, Y., Xia, L., Chen, W. Y., Shen, X. Y., He, T. J. and Xu, T. R.: Global aerosol change in the last decade: An analysis based on MODIS data, Atmos. Environ., 94, 680–686, doi:10.1016/j.atmosenv.2014.04.053, 2014.

Marais, E. A., Jacob, D. J., Jimenez, J. L., Campuzano-Jost, P., Day, D. A., Hu, W., Krechmer, J., Zhu, L., Kim, P. S., Miller, C. C., Fisher, J. A., Travis, K., Yu, K., Hanisco, T. F., Wolfe, G. M., Arkinson, H. L., Pye, H. O. T., Froyd, K. D., Liao, J. and McNeill, V. F.: Aqueous-phase mechanism for secondary organic aerosol formation from isoprene: application to the southeast United States and co-benefit of SO₂ emission controls, Atmos. Chem. Phys., 16(3), 1603–1618, doi:10.5194/acp-16-1603-2016, 2016.

Martin, R. V., Jacob, D. J., Yantosca, R. M., Chin, M. and Ginoux, P.: Global and regional decreases in tropospheric oxidants from photochemical effects of aerosols, J. Geophys. Res., 108(D3), 4097, doi:10.1029/2002JD002622, 2003.

Mauritsen, T.: Arctic climate change: Greenhouse warming unleashed, Nat. Geosci., 9(4), 271–272, doi:10.1038/ngeo2677, 2016.

Mehta, M., Singh, R., Singh, A., Singh, N. and Anshumali: Recent global aerosol optical depth variations and trends — A comparative study using MODIS and MISR level 3 datasets, Remote Sens. Environ., 181, 137–150, doi:10.1016/j.rse.2016.04.004, 2016.

de Meij, A., Pozzer, A. and Lelieveld, J.: Trend analysis in aerosol optical depths and pollutant emission estimates between 2000 and 2009, Atmos. Environ., 51, 75–85, doi:10.1016/j.atmosenv.2012.01.059, 2012.

Mielonen, T., Portin, H., Komppula, M., Leskinen, A., Tamminen, J., Ialongo, I., Hakkarainen, J., Lehtinen, K. E. J. and Arola, A.: Biomass burning aerosols observed in Eastern Finland during the Russian wildfires in summer 2010 – Part 2: Remote sensing, Atmos. Environ., 47, 279–287, doi:10.1016/j.atmosenv.2011.07.016, 2012.

Moosmüller, H., Chakrabarty, R. K. and Arnott, W. P.: Aerosol light absorption and its measurement: A review, J. Quant. Spectrosc. Radiat. Transf., 110(11), 844–878, doi:10.1016/j.jqsrt.2009.02.035, 2009.

Park, R. J., Jacob, D. J., Chin, M. and Martin, R. V.: Sources of carbonaceous aerosols over the United States and implications for natural visibility, J. Geophys. Res., 108(D12), 4355, doi:10.1029/2002JD003190, 2003.

Park, R. J., Jacob, D. J., Field, B. D., Yantosca, R. M. and Chin, M.: Natural and transboundary pollution influences on sulfate-nitrate-ammonium aerosols in the United States: Implications for policy, J. Geophys. Res., 109(D15), D15204, doi:10.1029/2003JD004473, 2004.

Penning de Vries, M. J. M., Beirle, S. and Wagner, T.: UV Aerosol Indices from SCIAMACHY: introducing the SCattering Index (SCI), Atmos. Chem. Phys., 9(24), 9555–9567, doi:10.5194/acp-9-9555-2009, 2009.

Penning de Vries, M. J. M., Beirle, S., Hörmann, C., Kaiser, J. W., Stammes, P., Tilstra, L. G., Tuinder, O. N. E. and Wagner, T.: A global aerosol classification algorithm incorporating multiple satellite data sets of aerosol and trace gas abundances, Atmos. Chem. Phys., 15(18), 10597–10618, doi:10.5194/acp-15-10597-2015, 2015.

Philip, S., Martin, R. V, Snider, G., Weagle, C. L., van Donkelaar, A., Brauer, M., Henze, D. K.,

754 Klimont, Z., Venkataraman, C., Guttikunda, S. K. and Zhang, Q.: Anthropogenic fugitive,
755 combustion and industrial dust is a significant, underrepresented fine particulate matter source in
756 global atmospheric models, Environ. Res. Lett., 12(4), 44018, doi:10.1088/1748-9326/aa65a4,
757 2017.

758 Pöschl, U.: Atmospheric Aerosols: Composition, Transformation, Climate and Health Effects,
759 Angew. Chemie Int. Ed., 44(46), 7520–7540, doi:10.1002/anie.200501122, 2005.

760 Pye, H. O. T., Liao, H., Wu, S., Mickley, L. J., Jacob, D. J., Henze, D. K. and Seinfeld, J. H.:
761 Effect of changes in climate and emissions on future sulfate-nitrate-ammonium aerosol levels in
762 the United States, J. Geophys. Res., 114(D1), D01205, doi:10.1029/2008JD010701, 2009.

763 Pye, H. O. T., Chan, A. W. H., Barkley, M. P. and Seinfeld, J. H.: Global modeling of organic
764 aerosol: the importance of reactive nitrogen (NO_x and
765 NO₃), Atmos. Chem. Phys., 10(22), 11261–11276, doi:10.5194/acp-10-
766 11261-2010, 2010.

767 Ramanathan, V. and Carmichael, G.: Global and regional climate changes due to black carbon,
768 Nat. Geosci., 1(4), 221–227, doi:10.1038/ngeo156, 2008.

769 Ridley, D. A., Heald, C. L. and Ford, B.: North African dust export and deposition: A satellite and
770 model perspective, J. Geophys. Res., 117(D2), D02202, doi:10.1029/2011JD016794, 2012.

771 Schepanski, K., Tegen, I., Laurent, B., Heinold, B. and Macke, A.: A new Saharan dust source
772 activation frequency map derived from MSG-SEVIRI IR-channels, Geophys. Res. Lett., 34(18),
773 L18803, doi:10.1029/2007GL030168, 2007.

774 Scollo, S., Kahn, R. A., Nelson, D. L., Coltelli, M., Diner, D. J., Garay, M. J. and Realmuto, V. J.:
775 MISR observations of Etna volcanic plumes, J. Geophys. Res. Atmos., 117(D6), n/a-n/a,
776 doi:10.1029/2011JD016625, 2012.

777 Shao, Y., Klose, M. and Wyrwoll, K.-H.: Recent global dust trend and connections to climate
778 forcing, J. Geophys. Res. Atmos., 118(19), 11,107-11,118, doi:10.1002/jgrd.50836, 2013.

779 Shi, W. and Wang, M.: Decadal changes of water properties in the Aral Sea observed by MODIS-
780 Aqua, J. Geophys. Res. Ocean., 120(7), 4687–4708, doi:10.1002/2015JC010937, 2015.

781 Shi, W., Wang, M. and Guo, W.: Long-term hydrological changes of the Aral Sea observed by
782 satellites, J. Geophys. Res. Ocean., 119(6), 3313–3326, doi:10.1002/2014JC009988, 2014.

783 Simon, H., Reff, A., Wells, B., Xing, J. and Frank, N.: Ozone Trends Across the United States
784 over a Period of Decreasing NOx and VOC Emissions, 2014.

785 Spivak, L., Terechov, A., Vitkovskaya, I., Batyrbayeva, M. and Orlovsky, L.: Dynamics of Dust
786 Transfer from the Desiccated Aral Sea Bottom Analysed by Remote Sensing, pp. 97–106,
787 Springer, Berlin, Heidelberg., 2012.

788 Spurr, R. J. D.: VLIDORT: A linearized pseudo-spherical vector discrete ordinate radiative
789 transfer code for forward model and retrieval studies in multilayer multiple scattering media, J.
790 Quant. Spectrosc. Radiat. Transf., 102(2), 316–342, doi:10.1016/j.jqsrt.2006.05.005, 2006.

791 Stier, P., Seinfeld, J. H., Kinne, S. and Boucher, O.: Aerosol absorption and radiative forcing,
792 Atmos. Chem. Phys., 7(19), 5237–5261, doi:10.5194/acp-7-5237-2007, 2007.

793 Storelvmo, T., Leirvik, T., Lohmann, U., Phillips, P. C. B. and Wild, M.: Disentangling greenhouse

warming and aerosol cooling to reveal Earth's climate sensitivity, Nat. Geosci., 9(4), 286–289, doi:10.1038/ngeo2670, 2016.

Torres, O., Bhartia, P. K., Herman, J. R., Ahmad, Z. and Gleason, J.: Derivation of aerosol properties from satellite measurements of backscattered ultraviolet radiation: Theoretical basis, J. Geophys. Res., 103(D14), 17099, doi:10.1029/98JD00900, 1998.

Torres, O., Tanskanen, A., Veihelmann, B., Ahn, C., Braak, R., Bhartia, P. K., Veefkind, P. and Levelt, P.: Aerosols and surface UV products from Ozone Monitoring Instrument observations: An overview, J. Geophys. Res., 112(D24), D24S47, doi:10.1029/2007JD008809, 2007.

Torres, O., Chen, Z., Jethva, H., Ahn, C., Freitas, S. R. and Bhartia, P. K.: OMI and MODIS observations of the anomalous 2008–2009 Southern Hemisphere biomass burning seasons, Atmos. Chem. Phys., 10(8), 3505–3513, doi:10.5194/acp-10-3505-2010, 2010.

Torres, O., Bhartia, P. K., Jethva, H. and Ahn, C.: Impact of the Ozone Monitoring Instrument Row Anomaly on the Long-term Record of Aerosol Products, Atmos. Meas. Tech., 1–25, doi:10.5194/amt-2017-429, 2018.

Travis, K. R., Jacob, D. J., Fisher, J. A., Kim, P. S., Marais, E. A., Zhu, L., Yu, K., Miller, C. C., Yantosca, R. M., Sulprizio, M. P., Thompson, A. M., Wennberg, P. O., Crounse, J. D., St. Clair, J. M., Cohen, R. C., Laughner, J. L., Dibb, J. E., Hall, S. R., Ullmann, K., Wolfe, G. M., Pollack, I. B., Peischl, J., Neuman, J. A. and Zhou, X.: Why do models overestimate surface ozone in the Southeast United States?, Atmos. Chem. Phys., 16(21), 13561–13577, doi:10.5194/acp-16-13561-2016, 2016.

Veefkind, J. P., Aben, I., McMullan, K., Förster, H., de Vries, J., Otter, G., Claas, J., Eskes, H. J., de Haan, J. F., Kleipool, Q., van Weele, M., Hasekamp, O., Hoogeveen, R., Landgraf, J., Snel, R., Tol, P., Ingmann, P., Voors, R., Kruizinga, B., Vink, R., Visser, H. and Levelt, P. F.: TROPOMI on the ESA Sentinel-5 Precursor: A GMES mission for global observations of the atmospheric composition for climate, air quality and ozone layer applications, Remote Sens. Environ., 120, 70–83, doi:10.1016/J.RSE.2011.09.027, 2012.

Wang, S., Zhang, Q., Martin, R. V, Philip, S., Liu, F., Li, M., Jiang, X. and He, K.: Satellite measurements oversee China's sulfur dioxide emission reductions from coal-fired power plants, Environ. Res. Lett., 10(11), 114015, doi:10.1088/1748-9326/10/11/114015, 2015.

Xing, J., Mathur, R., Pleim, J., Hogrefe, C., Gan, C.-M., Wong, D. C., Wei, C., Gilliam, R. and Pouliot, G.: Observations and modeling of air quality trends over 1990–2010 across the Northern Hemisphere: China, the United States and Europe, Atmos. Chem. Phys., 15(5), 2723–2747, doi:10.5194/acp-15-2723-2015, 2015.

Zhang, L., Henze, D. K., Grell, G. A., Torres, O., Jethva, H. and Lamsal, L. N.: What factors control the trend of increasing AAOD over the United States in the last decade?, J. Geophys. Res. Atmos., 122(3), 1797–1810, doi:10.1002/2016JD025472, 2017.

Zhao, B., Wang, S. X., Liu, H., Xu, J. Y., Fu, K., Klimont, Z., Hao, J. M., He, K. B., Cofala, J. and Amann, M.: NO x emissions in China: historical trends and future perspectives, Atmos. Chem. Phys, 13, 9869–9897, doi:10.5194/acp-13-9869-2013, 2013.

Figures

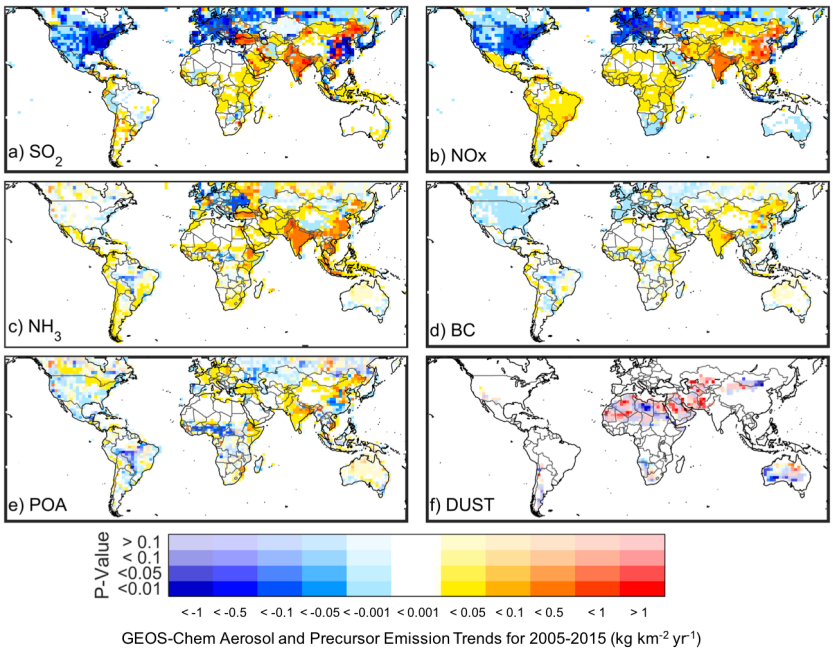

Figure 1: Trend in emissions of a) sulfur dioxide (SO_2) (kg SO_2 km^{-2} yr^{-1}), b) nitrogen oxides (NO_x) (kg NO km^{-2} yr^{-1}), ammonia (NH_3) (kg NH_3 km^{-2} yr^{-1}), black carbon (BC) (kg C km^{-2} yr^{-1}), primary organic carbon (POA) (kg C km^{-2} yr^{-1}), and dust (kg km^{-2} yr^{-1}) used in our GEOS-Chem simulation. The trends are calculated from the Generalized Least Squares regression of monthly time series values over 2005-2015.

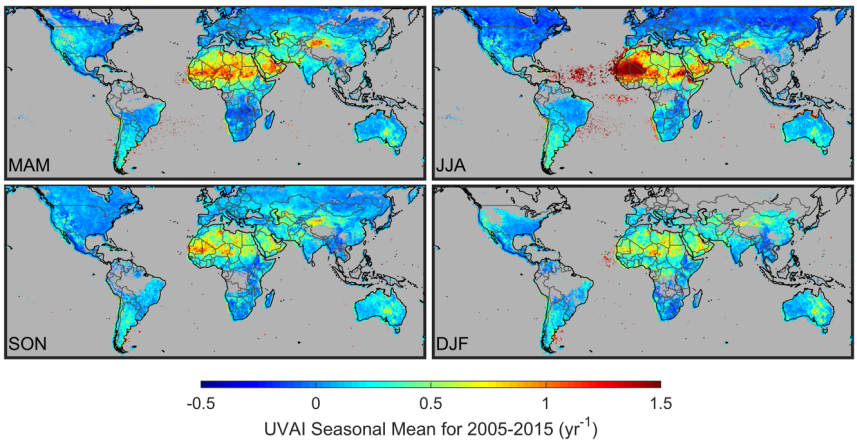

Figure 2: Seasonal mean UVAI values for the 2005-2015 period as observed by OMI for MAM (May, April, March), JJA (June, July August), SON (September, October, November), and DJF (December, January, February). Gray indicates persistent cloud fraction greater than 5%.

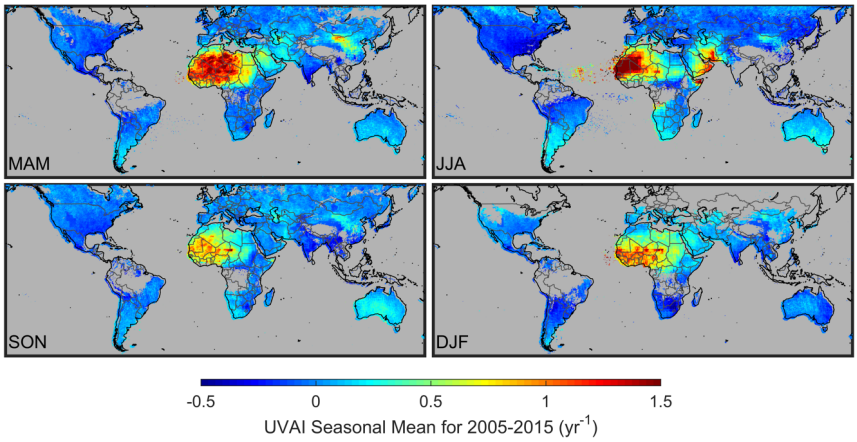

Figure 3: Seasonal mean UVAI values for the 2005-2015 period from our simulation coincidently sampled from OMI for MAM (May, April, March), JJA (June, July August), SON (September, October, November), and DJF (December, January, February). Gray indicates persistent cloud fraction greater than 5%.

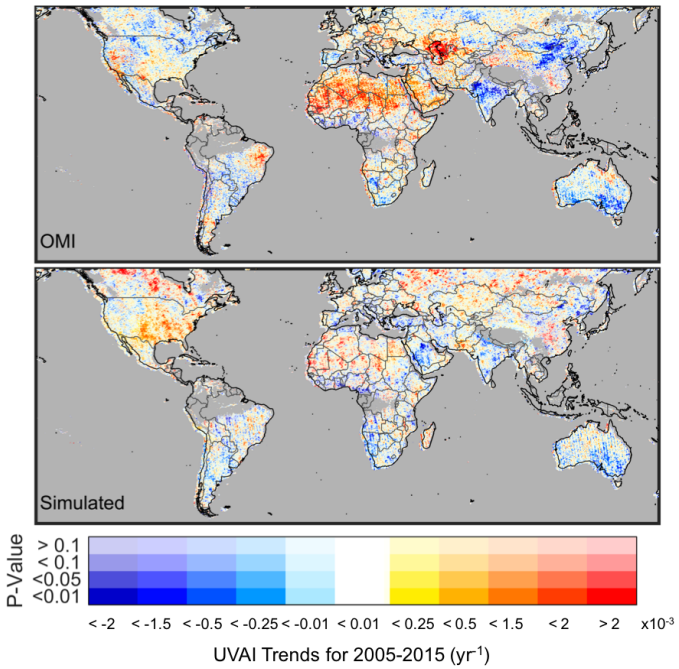

Figure 4: Trends in OMI (top panel) and simulated (bottom panel) UVAI values coincidently sampled from OMI calculated from the Generalized Least Squares regression of monthly time series values over 2005-2015. The opacity of the colors indicates the statistical significance of the trend. Gray indicates persistent cloud fraction greater than 5%.

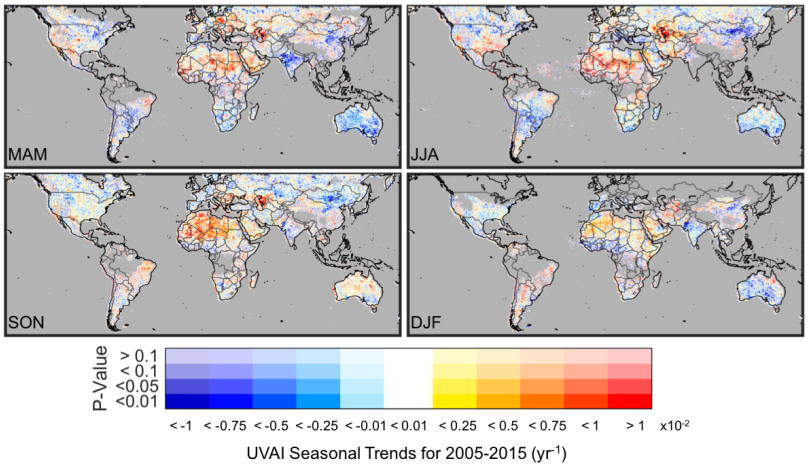

867

868 **Figure 5:** Seasonality of the trends in OMI UVAI values calculated from the Generalized Least
869 Squares regression of monthly time series values over 2005-2015 for MAM (May, April, March),
870 JJA (June, July August), SON (September, October, November), and DJF (December, January,
871 February). The opacity of the colors indicates the statistical significance of the trend. Gray
872 indicates persistent cloud fraction greater than 5%.

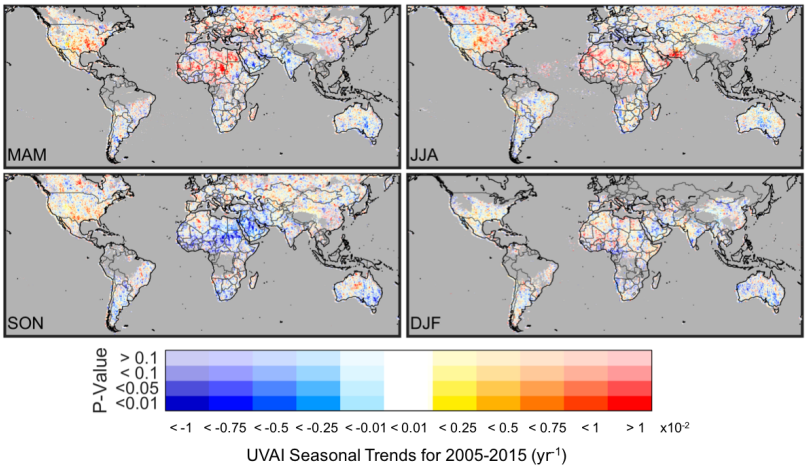

873

874 **Figure 6:** Seasonality of the trends in simulated UVAI values coincidently sampled from OMI
875 calculated from the Generalized Least Squares regression of monthly time series values over 2005-
876 2015 for MAM (May, April, March), JJA (June, July August), SON (September, October,
877 November), and DJF (December, January, February). The opacity of the colors indicates the
878 statistical significance of the trend. Gray indicates persistent cloud fraction greater than 5%.

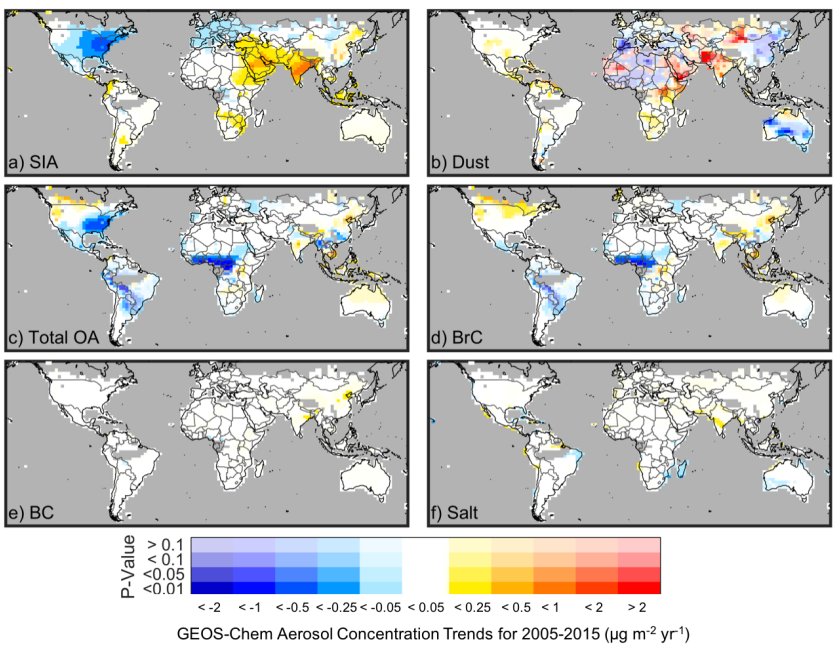

Figure 7: Trend in GEOS-Chem aerosol concentrations for a) secondary inorganic aerosol (SIA), b) dust, c) total organic aerosol (OA), d) brown carbon (BrC), e) black carbon (BC), and f) sea salt. The trends are calculated from the GLS regression of monthly aerosol concentration time series values over 2005-2015. The opacity of the colors indicates the statistical significance of the trend. Gray indicates persistent cloud fraction greater than 5%.

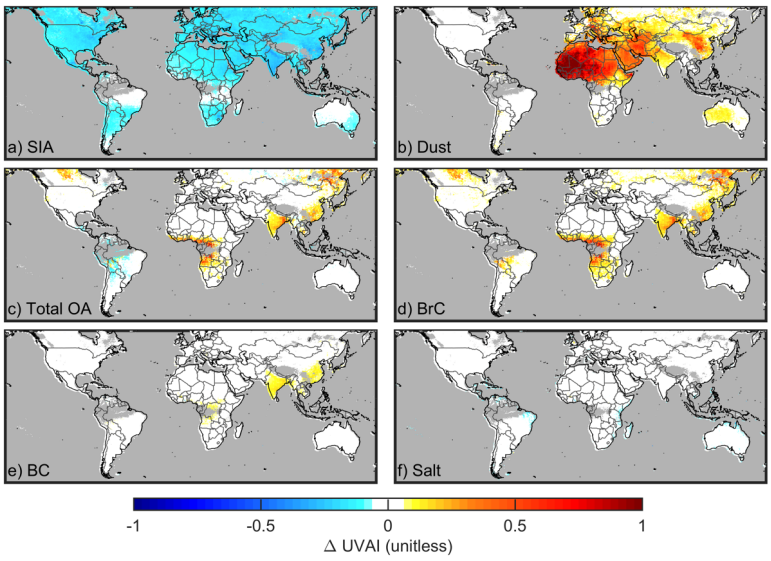

885

886 **Figure 8:** Annual mean change in simulated UVAI values for 2008 due to the doubling of
887 concentrations of a) secondary inorganic aerosol (SIA), b) dust, c) total organic aerosol (OA), d)
888 brown carbon (BrC), e) black carbon (BC), and f) sea salt from the GEOS-Chem simulation. Gray
889 indicates persistent cloud fraction greater than 5%.

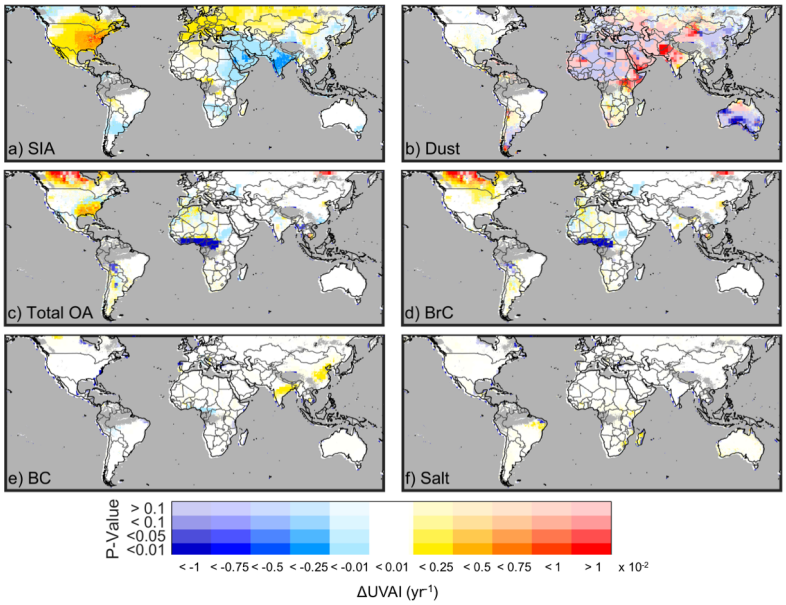

890

891 **Figure 9:** Change in simulated UVAI values due to the 2005-2015 trends in a) secondary inorganic
892 aerosols (SIA), b) dust, c) total organic aerosol (OA), d) brown carbon (BrC), e) black carbon
893 (BC), and f) sea salt from the GEOS-Chem simulation. Gray indicates persistent cloud fraction
894 greater than 5%.